Theory of light detection in the presence of feedback

J. H. Shapiro, G. Saplakoglu, and S.-T. Ho

Department of Electrical Engineering and Computer Science, Research Laboratory of Electronics, Massachusetts Institute of Technology, Cambridge, Massachusetts 02139

P. Kumar

Department of Electrical Engineering and Computer Science, Northwestern University, Evanston, Illinois 60201

B. E. A. Saleh

Columbia Radiation Laboratory, Department of Electrical Engineering, Columbia University, New York, New York 10027

M. C. Teich

Center for Telecommunications Research, Department of Electrical Engineering, Columbia University, New York, New York 10027

Received December 31, 1986; accepted April 27, 1987

The usual open-loop quantum and semiclassical theories of light detection are extended to include closed-loop operation in which there is feedback from the detector to the source. It is shown that the unmistakable signatures of nonclassical light associated with open-loop detection, such as sub-shot-noise spectra and sub-Poisson photocounts, do not carry over to closed-loop systems. This behavior is illustrated through quantitatively indistinguishable quantum and semiclassical analyses of two recent closed-loop experiments in which sub-Poisson photocount statistics were produced. It turns out that if the open-loop illumination does not require the use of quantum photodetection theory, then neither does the closed-loop illumination. Conversely, if the open-loop illumination is nonclassical, then the closed-loop behavior must be analyzed quantum mechanically. The use of nonclassical field correlations to obtain light beams that give sub-Poisson open-loop photocounts from these closed-loop arrangements is discussed and generalized into a synthesis procedure for producing light beams with arbitrary open-loop photocount statistics.

1. INTRODUCTION

The usual formulations of the quantum[1–5] and semiclassical[5–8] theories of photodetection presume open-loop configurations, i.e., that there are no feedback paths leading from the output of the photodetector to the light beam impinging on that detector. In such configurations, the qualitative and quantitative distinctions between the quantum and semiclassical theories are well understood. In the quantum theory, photocurrent and photocount randomness arise from the quantum noise in the illumination beam, whereas in the semiclassical theory the fundamental source of randomness is associated with the excitations of the atoms forming the detector. Nevertheless, the quantum theory subsumes the semiclassical theory in a natural way in that their open-loop predictions coincide exactly when the quantum field illuminating the photodetector in the former approach is in a classical state, i.e., a Glauber coherent state or a classically random mixture of such states.[3–5] Inasmuch as it is only recently,[9–15] and with some difficulty, that light beams have been generated whose quantum statistics fall outside the classical states, it is not surprising that the semiclassical theory has continued to be the mainstay of photodetection sensitivity calculations.

The clarity of understanding associated with open-loop photodetection does not extend to closed-loop configurations in which there is a feedback path leading from the output of the detector back to the light beam at the detector input. In this paper, we develop the quantum and semiclassical theories of light detection for closed-loop configurations.[16] The fundamental quantity of interest in these theories is the random point process formed by the photodetection event times. Thus we begin, in Section 2, with a high-level review of such processes, focusing on their application to open-loop photodetection. In particular, we introduce the doubly stochastic Poisson process (DSPP)[17,18] of semiclassical open-loop theory[5–8] and the more general self-exciting point process (SEPP)[17,18] of quantum open-loop theory.[3] This material both establishes the analytical framework that we need for the closed-loop treatment and summarizes the semiclassical limits and nonclassical signatures of open-loop operation.

Our analysis of closed-loop photodetection begins in Section 3. Here we use the incremental point-process descriptor from Section 2 to show that both the semiclassical and quantum theories lead to SEPP's for the closed-loop case. As a result, the unmistakable open-loop signatures of nonclassical light, such as sub-shot-noise spectra and sub-Pois-

0740-3224/87/101604-17$02.00

son photocounts, do not carry over to closed-loop systems. We illustrate this behavior by providing quantitatively indistinguishable quantum and semiclassical explanations for two recent closed-loop experiments in which sub-Poisson photocounts were produced.[19–21] There is, nevertheless, a vital distinction between the two theories as applied to these experiments. According to the quantum theory, nonclassical open-loop beams can be extracted from these closed-loop arrangements by augmenting them to exploit the nonclassical light-beam correlations associated with photon twins[22,23] or Kerr-effect quantum nondemolition (QND) measurements.[21,24] Indeed, the former approach was recently used to produce a nonclassical open-loop beam.[25] We address these field-extraction procedures in Section 4 and show that they can be generalized to a schema for synthesizing light beams of arbitrary photocount statistics.

2. POINT PROCESSES AND OPEN-LOOP PHOTODETECTION

For the purposes of this paper, the general photodetection construct of interest, be it semiclassical or quantum, open or closed loop, takes the form shown in Fig. 1. A quasi-monochromatic paraxial scalar light beam of nominal frequency ν_0 illuminates the active region of the photodetector.[26] The quantities of interest at the detector output are the photocurrent i_t and the photocount record N_t. The former is a train of impulses (each of area q, with q the electron charge) located at the photodetection event times $\{t_i\}$.[27] The latter counts the number of such events that have occurred in the time interval $[0, t)$ and is given by

$$N_t = q^{-1}\int_0^t i_\tau d\tau. \tag{1}$$

The event times $\{t_i\}$ that underlie both i_t and N_t comprise a random point process. For convenience, they will be arranged in increasing order with t_1 denoting the first event in the interval $[0, \infty)$, as sketched in Fig. 2.

A. Point-Process Statistics

Without loss of generality, we shall confine ourselves to point processes that are conditionally orderly[17]; in essence, this means that events occur one at a time. More precisely, with

$$\Delta N_t \equiv N_{t+\Delta t} - N_t \tag{2}$$

being the number of events that occur during $[t, t + \Delta t)$, a point process is conditionally orderly if its incremental probabilities obey

$$\lim_{\Delta t\to 0} \Delta t^{-1}[1 - \Pr(\Delta N_t = 0|\mathbf{t}_t, N_t)] = \mu_t, \tag{3}$$

$$\lim_{\Delta t\to 0} \Delta t^{-1}\Pr(\Delta N_t = 1|\mathbf{t}_t, N_t) = \mu_t, \tag{4}$$

and

$$\lim_{\Delta t\to 0} \Delta t^{-1}\Pr(\Delta N_t \geq 2|\mathbf{t}_t, N_t) = 0, \tag{5}$$

where $\mathbf{t}_t \equiv (t_1, t_2, \ldots, t_{N_t})$ is the vector of event times occurring in $[0, t)$. Physically, μ_t (called the conditional rate function) is the conditional probability per unit time for there to be an event at t, given the history of the process up to t.[28] In general, μ_t may be an arbitrary nonnegative function of $\{\mathbf{t}_t, N_t\}$, in which case Eqs. (3)–(5) constitute the incremental statistical generator of the general SEPP.[17,18] In its simplest form, μ_t does not depend on the event history, and Eqs. (3)–(5) then describe the Poisson process with rate function μ_t. Of interest in the sequel is the DSPP, whose incremental statistics are given by Eqs. (3)–(5) with[17,18]

$$\mu_t = \langle \lambda_t|\mathbf{t}_t, N_t\rangle, \tag{6}$$

where angle brackets denote expectation and λ_t is a nonnegative random process that is not directly influenced by the point process, i.e., λ_t is conditionally independent of $\{\mathbf{t}_t, N_t\}$ given knowledge of $\{\lambda_\tau\colon\ \tau < t\}$. As its name implies, the DSPP is a Poisson process whose rate function is the random process λ_t. It is worth noting here that the class of SEPP's is known to be broader than that of DSPP's; this point will be illustrated below in the context of open-loop photodetection.

A useful alternative specification of point-process statistics can be made through multicoincidence rates (MCR's).[2,3,17] The kth-order MCR is

$$w_k(\tau_1, \tau_2, \ldots, \tau_k) = \lim_{\Delta t\to 0} (\Delta t)^{-k}\Pr\left(\prod_{i=1}^{k}\Delta N_{\tau_i} = 1\right) \tag{7}$$

for $k = 1, 2, \ldots$. Basically, $w_k(\tau_1, \tau_2, \ldots, \tau_k)\Delta t^k$ is the probability that events are registered within Δt intervals about the distinct times $\tau_1, \tau_2, \ldots, \tau_k$. No ordering is implied among the $\{\tau_i\}$, nor is the possibility of additional events excluded. For a Poisson process with rate function μ_t, we have that

$$w_k(\tau_1, \tau_2, \ldots, \tau_k) = \prod_{i=1}^{k}\mu_{\tau_i}; \tag{8}$$

for a DSPP with random rate function λ_t we have that

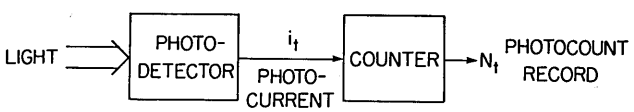

Fig. 1. Generic photodetection configuration.

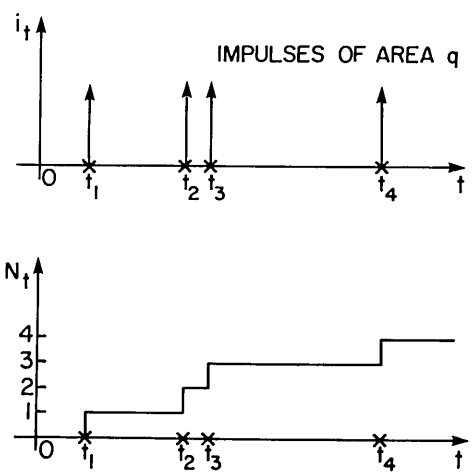

Fig. 2. Pictorial of relationships between the photodetection event times $\{t_i\}$, the photocurrent i_t, and the photocount record N_t.

$$w_k(\tau_1, \tau_2, \ldots, \tau_k) = \left\langle \prod_{i=1}^{k} \lambda_{\tau_i} \right\rangle. \tag{9}$$

There is a more general result connecting MCR's to conditional rate functions for arbitrary SEPP's, but it is not sufficiently explicit to warrant inclusion here.[17]

In terms of the MCR's, we have the following results for the photocount and photocurrent statistics associated with the point process $\{t_i\}$. The count probability distribution is

$$\Pr(N_t = n) = \sum_{m=n}^{\infty} \frac{(-1)^{m-n}}{(m-n)!n!} \int_0^t d\tau_1 \int_0^t d\tau_2 \ldots \int_0^t d\tau_m w_m(\tau_1, \tau_2, \ldots, \tau_m); \tag{10}$$

it has a mean

$$\langle N_t \rangle = \int_0^t w_1(\tau) d\tau \tag{11}$$

and a variance

$$\mathrm{var}(N_t) = \langle N_t \rangle + \int_0^t d\tau \int_0^t d\tau' [w_2(\tau, \tau') - w_1(\tau) w_1(\tau')]. \tag{12}$$

For a stationary point process w_1 is a constant and w_2 depends only on the difference between its arguments. In this case the mean photocurrent is

$$\langle i \rangle = q w_1, \tag{13}$$

and its noise spectrum (bilateral covariance spectrum) is

$$S_{ii}(f) = q \langle i \rangle + q^2 \int_{-\infty}^{\infty} d\tau [w_2(\tau) - w_1^2] \exp(-i2\pi f\tau). \tag{14}$$

Equations (10)–(12) reduce to the familiar Poisson limits when the MCR's are given by Eq. (8). Their behavior for DSPP's and SEPP's forms the core of our overview of open-loop photodetection.

B. Open-Loop Photodetection

In the open-loop semiclassical theory, the event times underlying both i_t and N_t form a DSPP with random rate function given by

$$\lambda_t = \eta P_t / h\nu_0, \tag{15}$$

in terms of the detector quantum efficiency η, the (possibly random) power illuminating the detector P_t, and the photon energy $h\nu_0$. Equations (9) and (10) then yield Mandel's rule[6] for the count probability distribution

$$\Pr(N_t = n) = \left\langle \frac{W^n e^{-W}}{n!} \right\rangle, \tag{16}$$

where

$$W \equiv \int_0^t d\tau \eta P_\tau / h\nu_0. \tag{17}$$

It is well known that this distribution does not permit sub-Poisson behavior, viz., from Eqs. (9), (11), (12), (15), (17),

$$\mathrm{var}(N_t) = \langle N_t \rangle + \mathrm{var}(W) \geq \langle N_t \rangle, \tag{18}$$

with equality if and only if W is nonrandom. If P_t is a stationary random process with mean $\langle P \rangle$ and noise spectrum $S_{PP}(f)$, then our DSPP formulas yield

$$\langle i \rangle = q\eta \langle P \rangle / h\nu_0 \tag{19}$$

and

$$S_{ii}(f) = q \langle i \rangle + (q\eta / h\nu_0)^2 S_{PP}(f) \tag{20}$$

for the like statistics of the photocurrent. Here we see the well-known shot-noise lower limit of semiclassical photodetection, i.e.,

$$S_{ii}(f) \geq q \langle i \rangle, \tag{21}$$

with equality at all frequencies only if P_t equals $\langle P \rangle$ with probability one.

In the open-loop quantum theory, the event times underlying i_t and N_t form a SEPP whose kth-order MCR is

$$w_k(\tau_1, \tau_2, \ldots, \tau_k) = \eta^k \mathrm{Tr}\left\{ \hat{\rho} \int_{A_d} d\mathbf{x}_1 \ldots \int_{A_d} d\mathbf{x}_k \times \left[\prod_{i=1}^{k} \hat{E}^\dagger(\mathbf{x}_i, \tau_i) \right] \left[\prod_{i=1}^{k} \hat{E}(\mathbf{x}_i, \tau_i) \right] \right\}, \tag{22}$$

where $\hat{\rho}$ is the density operator for the field, $\hat{E}(\mathbf{x}, t) \exp(-i2\pi\nu_0 t)$ is the positive-frequency photon-units field operator for $\mathbf{x} = (x, y)$ in the plane of the photodetector,[29] and A_d represents the active area of the photodetector. When $\hat{\rho}$ is a classical state, it has a proper P representation, namely,

$$\hat{\rho} = \int d^2\alpha \, P(\alpha; \alpha^*) |\alpha\rangle \langle\alpha| \tag{23}$$

for P a classical probability density and $|\alpha\rangle$ the multimode coherent state. Equation (22) then becomes

$$w_k(\tau_1, \tau_2, \ldots, \tau_k) = \int d^2\alpha P(\alpha; \alpha^*) \prod_{i=1}^{k} (\eta P_{\tau_i} / h\nu_0), \tag{24}$$

where

$$P_t = h\nu_0 \langle\alpha| \int_{A_d} d\mathbf{x} \hat{E}^\dagger(\mathbf{x}, t) \hat{E}(\mathbf{x}, t) |\alpha\rangle \tag{25}$$

is a nonnegative classical stochastic process whose statistics are specified by $P(\alpha; \alpha^*)$, and all the semiclassical formulas are reproduced. States that do not have proper P representations are called nonclassical. Their photocount and photocurrent statistics require SEPP's that, in general, are not DSPP's. For example, if $\hat{\rho}$ is a photon eigenstate that has exactly N photons within the space–time region $A_d \times [0, T)$, then Eqs. (10) and (22) yield the binomial distribution[2,3,30]

$$\Pr(N_T = n) = \binom{N}{n} \eta^n (1-\eta)^{N-n} \tag{26}$$

for $n = 0, 1, 2, \ldots, N$. This distribution is sub-Poissonian for all $0 < \eta \leq 1$ and collapses to the expected nonrandom behavior as the quantum efficiency goes to unity.[30,31]

Sub-Poisson photocounts and sub-shot-noise photocurrent spectra provide unmistakable signatures for nonclassical light in open-loop photodetection. Such effects have now been observed in a variety of experiments. Short and

Mandel[10] produced conditionally sub-Poisson light by means of resonance fluorescence from sodium vapor. Their experiment required that the starting time of the photocounting interval coincide with the entry of a single atom into the field of view of the apparatus and that the light be generated only by a single atom. Subsequently, Teich and Saleh[11] produced unconditionally (continuous-wave) sub-Poisson light by using a space-charge-limited electron beam to excite the Franck–Hertz effect in mercury vapor. More recently, Slusher *et al.*,[12] Shelby *et al.*,[13] and Maeda *et al.*[15] have seen sub-shot-noise photocurrent spectra in homodyne detection of light that has undergone four-wave mixing, as have Wu *et al.*[14] in a three-wave mixing experiment. It is relevant to note that self-exciting point processes play a role in all these cases. In the Short–Mandel experiment, the self-excitation is provided by the dead time associated with successive atomic emissions.[10] In the Teich–Saleh experiment, it is provided by the space charge associated with the electron beam. Indeed, they modeled[32] the statistics of this beam as a renewal point process, which of course, is a special kind of SEPP. Self-excitation, in the multiwave mixing experiments, can be attributed to the quantum correlations between the pump and probe beams produced by photon exchanges occurring through the nonlinear optical process.

3. CLOSED-LOOP PHOTODETECTION

Most theoretical results for open-loop systems do not carry over to closed-loop photodetection. We proceed now to reexamine the semiclassical and quantum photodetection properties of i_t and N_t when the output of the photodetector is permitted to affect the light at its input through a causal, but possibly nonlinear, feedback loop, as shown in Fig. 3. In both the semiclassical and quantum formulations it then turns out that the photodetection event times form a SEPP. Semiclassically, this is most easily seen through the incremental point-process description [Eqs. (3)–(5)]. In the absence of feedback we have a DSPP, i.e., the semiclassical conditional rate obeys

$$\mu_t = \langle \eta P_t/h\nu_0 | \mathbf{t}_t, N_t \rangle, \tag{27}$$

where P_t, the illumination power, is a nonnegative random process that is not directly influenced by the point process, viz., P_t is conditionally independent of the photocount history $\{\mathbf{t}_t, N_t\}$ given its own history $\{P_\tau : \tau < t\}$. Closing the feedback loop leaves Eq. (27) formally intact but makes

$$P_t = P_t(\{\mathbf{t}_t, N_t\}) \tag{28}$$

an explicit function of the photocount history. Thus the DSPP condition is violated, indicating that closed-loop semiclassical photodetection leads, in general, to a SEPP.

Quantum mechanically, open-loop photodetection already requires SEPP descriptions; passing to the closed-loop configuration modifies many of the detailed results but does not break out of the general SEPP structure. For example, in the open-loop configuration it is known[4,5] that the photocurrent i_t realizes the quantum measurement[33]

$$\hat{i}_t \equiv q \int_{A_d} d\mathbf{x} \hat{E}'^{\dagger}(\mathbf{x}, t) \hat{E}'(\mathbf{x}, t), \tag{29}$$

with

$$\hat{E}'(\mathbf{x}, t) \equiv \eta^{1/2} \hat{E}(\mathbf{x}, t) + (1 - \eta)^{1/2} \hat{E}_v(\mathbf{x}, t), \tag{30}$$

where $\hat{E}_v(\mathbf{x}, t)$ is a vacuum-state field operator representing subunity quantum efficiency noise. In Eqs. (29) and (30), $\hat{E}(\mathbf{x}, t)$ and $\hat{E}_v(\mathbf{x}, t)$ are commuting free-field operators that do not explicitly depend on $\{i_\tau : \tau < t\}$. When the loop is closed, Eqs. (29) and (30) continue to apply but with $\hat{E}(\mathbf{x}, t)$ explicitly dependent on past measurements.

Because both the semiclassical and quantum theories lead to SEPP's, there are no unmistakable signatures for nonclassical light in the closed loop. To be specific, for a SEPP the quantity $w_2(t, s) - w_1(t)w_1(s)$ need not be positive semidefinite, so that [see Eqs. (12) and (14)] sub-Poisson photocounts and sub-shot-noise photocurrent spectra are possible in both theories. In what follows, we shall explore this behavior for two feedback configurations, which we term the dead-time-modified Poisson process (DTMPP) and the negative-linear-feedback process (NLFP).

A. Dead-Time-Modified Poisson Process

It has long been known that semiclassical photocounting statistics are impacted by dead time in the detection system. Consider the nonparalyzable DTMPP, which is a renewal process and hence a SEPP.[17,34–36] For a detector with fixed dead time τ_d, illuminated, in the semiclassical theory, by nonrandom light of constant power P, the photocount probability distribution is[35,36]

$$\Pr(N_t = n) = \begin{cases} \sum_{k=0}^{n} p_0[k, \lambda(t - n\tau_d)] - \sum_{k=0}^{n-1} p_0\{k, \lambda[t - (n-1)\tau_d]\} & \text{for } n < t/\tau_d \\ 1 - \sum_{k=0}^{n-1} p_0\{k, \lambda[t - (n-1)\tau_d]\} & \text{for } t/\tau_d \le n < t/\tau_d + 1, \\ 0 & \text{for } n \ge t/\tau_d + 1 \end{cases} \tag{31}$$

where

$$p_0(k, a) \equiv a^k e^{-a}/k!, \qquad \lambda \equiv \eta P/h\nu_0. \tag{32}$$

These results are valid for a detector that is unblocked at the beginning of each counting interval, although exact number distributions for counters that are blocked and for equilibri-

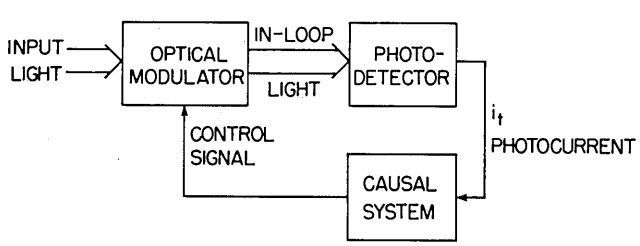

Fig. 3. Closed-loop photodetection configuration.

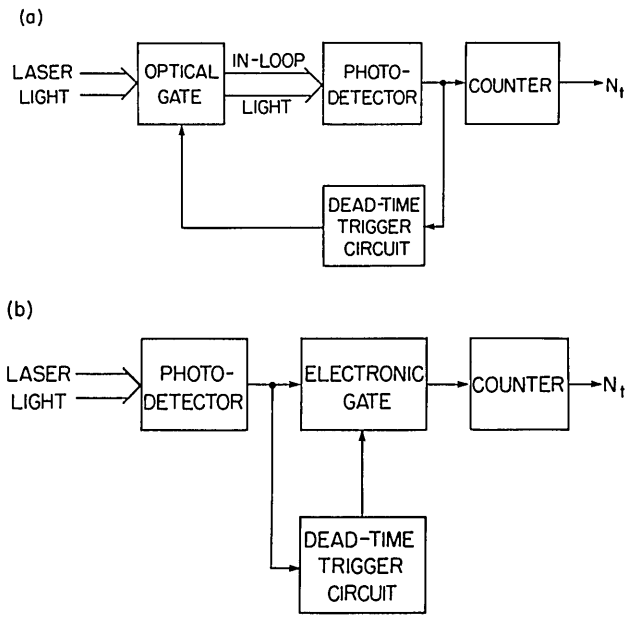

Fig. 4. (a) Closed-loop photocounting experiment carried out by Walker and Jakeman.[19] (b) Photocounting experiment carried out by Teich and Vannucci.[36]

um counters are also available. In the usual situation, the mean count is much greater than unity, in which case the differences arising from the three initial conditions are insubstantial and a simple approximation for the photocount distribution suffices.[36] The photocount mean and variance then take the asymptotic forms

$$\langle N_t \rangle = \lambda t/(1 + \lambda\tau_d) \tag{33}$$

and

$$\mathrm{var}(N_t) = \langle N_t \rangle/(1 + \lambda\tau_d)^2, \tag{34}$$

representing sub-Poisson behavior for all values of $\lambda\tau_d$.

The DTMPP results are relevant to experiments recently carried out by Walker and Jakeman.[19] The simplest form of their experimental arrangement is illustrated in Fig. 4(a). The registration of a photoevent at the detector operates a trigger circuit that causes an optical gate to be closed for a fixed period of time τ_d after the time of registration. During this period, the power P_t of the (He–Ne) laser illuminating the detector is set precisely equal to zero so that no photodetections are registered. The arrangement is therefore equivalent to the one illustrated in Fig. 4(b), in which the gating is electronic rather than optical, at least so far as the photocount statistics are concerned. This latter arrangement was used by Teich and Vannucci,[36] and sub-Poisson photocounts were observed in both cases. This is because the point process seen by the counter in these experiments is the DTMPP considered above. As Walker and Jakeman understood, their observations can be explained without recourse to the quantum theory of photodetection; under closed-loop conditions, sub-Poisson photocounts are possible within the semiclassical framework. Nevertheless, it is instructive to develop the quantum foundations for Eqs. (33) and (34) in a manner conducive to generalization.

Consider the quantum version of a somewhat richer dead-time experiment shown in Fig. 5. Here, a coherent-state signal field $\hat{E}_S(\mathbf{x}, t)$ with mean

$$\langle \alpha|\hat{E}_S(\mathbf{x}, t)|\alpha\rangle = (P/h\nu_0 A_d)^{1/2} \tag{35}$$

illuminates an in-loop photodetector of quantum efficiency η through a feedback-controlled flip mirror. For τ_d sec after each in-loop photocount registration, the flip mirror directs $\hat{E}_S(\mathbf{x}, t)$ to an out-of-loop photodetector of matched quantum efficiency η. During this dead-time interval, the in-loop detector is illuminated by a vacuum-state field operator $\hat{E}_M(\mathbf{x}, t)$. After this dead-time interval the mirror returns to its previous position, in which $\hat{E}_S$ illuminates the in-loop detector and $\hat{E}_M$ illuminates the out-of-loop detector.

We derive the steady-state first and second moments (means, variances, and covariance) of the in-loop and out-of-loop photocount records N_t and N_t' in the high-mean-count limit. Toward that end, we recast the flip-mirror subsystem into the explicit lossless modulated beam-splitter form, shown in Fig. 6, in which

$$\hat{E}_{\mathrm{IN}}(\mathbf{x}, t) = [T(t)]^{1/2}\hat{E}_S(\mathbf{x}, t) + [1 - T(t)]^{1/2}\hat{E}_M(\mathbf{x}, t) \tag{36}$$

and

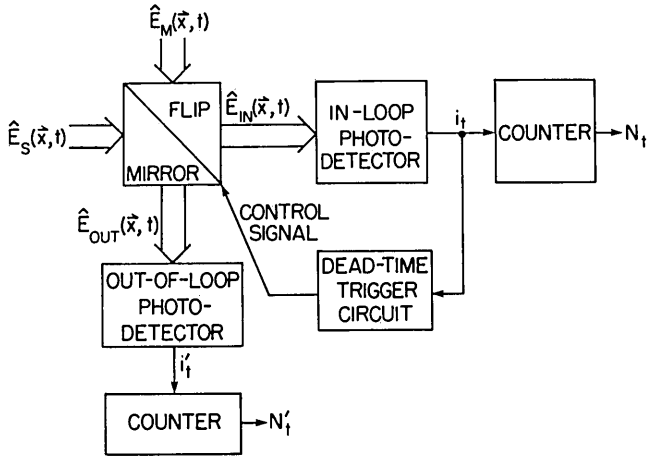

Fig. 5. Quantum-photodetection configuration that can be used to represent the DTMPP experiments carried out by Walker and Jakeman.[19]

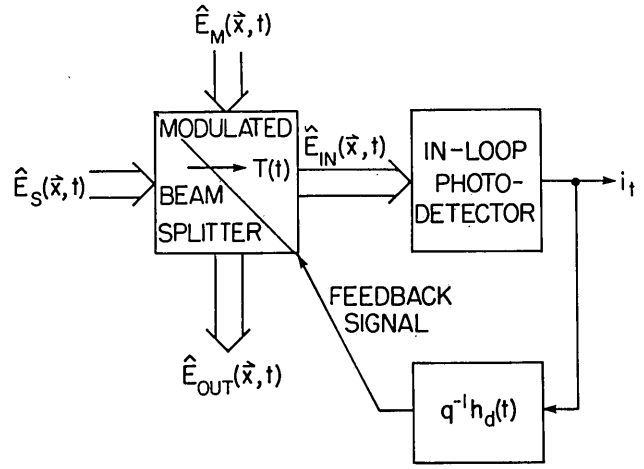

Fig. 6. Modulated beam-splitter version of the flip-mirror subsystem from Fig. 5; the beam splitter's intensity transmission obeys $T(t) = 1 - q^{-1}\int i_r h_d(t - \tau)\mathrm{d}\tau$, with $h_d(t) = 1$ for $0 < t \leq \tau_d$.

$$\hat{E}_{\mathrm{OUT}}(\mathbf{x}, t) = -[1 - T(t)]^{1/2}\hat{E}_S(\mathbf{x}, t) + [T(t)]^{1/2}\hat{E}_M(\mathbf{x}, t), \quad (37)$$

with beam-splitter transmission given by

$$T(t) = 1 - q^{-1}\int i_\tau h_d(t - \tau)\mathrm{d}\tau \quad (38)$$

in terms of the causal linear system impulse response

$$h_d(t) = \begin{cases} 1 & \text{for } 0 < t \le \tau_d \\ 0 & \text{otherwise} \end{cases}. \quad (39)$$

Because i_t has an impulse of area q at each in-loop photoevent and because such events are impossible when the in-loop detector is illuminated by the vacuum-state field $\hat{E}_M$, it is easily verified that Eqs. (36)–(39) correctly describe the flip-mirror arrangement.

To proceed further, we replace the classical in-loop and out-of-loop photocurrents i_t and i_t' by their associated operator representations [cf. Eqs. (29), (30)]:

$$\hat{i}_t = q\int_{A_d} \mathrm{d}\mathbf{x}\hat{E}_{\mathrm{IN}}{}'^{\dagger}(\mathbf{x}, t)\hat{E}_{\mathrm{IN}}{}'(\mathbf{x}, t) \quad (40)$$

and

$$\hat{i}_t{}' = q\int_{A_d} \mathrm{d}\mathbf{x}\hat{E}_{\mathrm{OUT}}{}'^{\dagger}(\mathbf{x}, t)\hat{E}_{\mathrm{OUT}}{}'(\mathbf{x}, t), \quad (41)$$

where

$$\hat{E}_j'(\mathbf{x}, t) = \eta^{1/2}\hat{E}_j(\mathbf{x}, t) + (1 - \eta)^{1/2}\hat{E}_{jv}(\mathbf{x}, t) \quad (42)$$

for j = IN, OUT, and $\{\hat{E}_{\mathrm{IN}v}, \hat{E}_{\mathrm{OUT}v}\}$ are vacuum-state field operators. We next employ the high-mean-count condition to justify the following linearization[37] of Eqs. (36)–(38):

$$\langle\hat{E}_{\mathrm{IN}}\rangle \approx \langle T\rangle^{1/2}\langle\hat{E}_S\rangle = (\langle T\rangle P/h\nu_0 A_d)^{1/2}, \quad (43)$$

$$\begin{aligned}\Delta\hat{E}_{\mathrm{IN}}(\mathbf{x}, t) &\equiv \hat{E}_{\mathrm{IN}}(\mathbf{x}, t) - \langle\hat{E}_{\mathrm{IN}}\rangle \\ &\approx \langle T\rangle^{1/2}\Delta\hat{E}_S(\mathbf{x}, t) + (1 - \langle T\rangle)^{1/2}\hat{E}_M(\mathbf{x}, t) \\ &\quad + [\Delta\hat{T}(t)/2\langle T\rangle^{1/2}]\langle\hat{E}_S\rangle, \end{aligned} \quad (44)$$

$$\langle\hat{E}_{\mathrm{OUT}}\rangle \approx -(1 - \langle T\rangle)^{1/2}\langle\hat{E}_S\rangle, \quad (45)$$

$$\begin{aligned}\Delta\hat{E}_{\mathrm{OUT}}(\mathbf{x}, t) &\approx -(1 - \langle T\rangle)^{1/2}\Delta\hat{E}_S(\mathbf{x}, t) + \langle T\rangle^{1/2} \\ &\quad \times \hat{E}_M(\mathbf{x}, t) + [\Delta\hat{T}(t)/2(1 - \langle T\rangle)^{1/2}]\langle\hat{E}_S\rangle, \end{aligned} \quad (46)$$

$$\begin{aligned}\langle T\rangle &\approx 1 - \int \eta A_d\langle\hat{E}_{\mathrm{IN}}\rangle^2 h_d(t - \tau)\mathrm{d}\tau \\ &= 1 - \eta A_d\langle\hat{E}_{\mathrm{IN}}\rangle^2\tau_d, \end{aligned} \quad (47)$$

and

$$\begin{aligned}\Delta\hat{T}(t) \approx -\int 2\eta^{1/2}\langle\hat{E}_{\mathrm{IN}}\rangle\mathrm{Re}\Big\{\int_{A_d}\mathrm{d}\mathbf{x}[\eta^{1/2}\Delta\hat{E}_{\mathrm{IN}}(\mathbf{x}, \tau) \\ + (1 - \eta)^{1/2}\hat{E}_{\mathrm{IN}v}(\mathbf{x}, \tau)]\Big\}h_d(t - \tau)\mathrm{d}\tau. \end{aligned} \quad (48)$$

The equations for the mean values are easily solved, yielding

$$\langle\hat{E}_{\mathrm{IN}}\rangle = \{(P/h\nu_0 A_d)/[1 + (\eta P\tau_d/h\nu_0)]\}^{1/2}, \quad (49)$$

$$\langle\hat{E}_{\mathrm{OUT}}\rangle = -[(P/h\nu_0 A_d) - \langle\hat{E}_{\mathrm{IN}}\rangle^2]^{1/2}, \quad (50)$$

from which it follows that

$$\begin{aligned}\langle N_t\rangle &= q^{-1}\int_0^t \langle i_\tau\rangle\,\mathrm{d}\tau \approx \eta\langle\hat{E}_{\mathrm{IN}}\rangle^2 A_d t \\ &= \lambda t/(1 + \lambda\tau_d) \end{aligned} \quad (51)$$

and

$$\begin{aligned}\langle N_t'\rangle &= q^{-1}\int_0^t \langle i_\tau'\rangle\,\mathrm{d}\tau \approx \eta\langle\hat{E}_{\mathrm{OUT}}\rangle^2 A_d t \\ &= \lambda t - \lambda t/(1 + \lambda\tau_d), \end{aligned} \quad (52)$$

where $\lambda = \eta P/h\nu_0$, as in Eqs. (31)–(34). Equation (51) reproduces Eq. (33), as promised. Equation (52) is, in fact, self-evident in that, by construction, $N_t + N_t'$ corresponds to performing quantum efficiency η photocounting on the coherent-state field $\hat{E}_S$. Thus $N_t + N_t'$ must be a Poisson process of rate λ. The less obvious results concern the second moments, with which we deal below.

By using the high-mean-count linearization we know that

$$\mathrm{var}(N_t) \approx 4\eta A_d\langle\hat{E}_{\mathrm{IN}}\rangle^2\left\langle\left[\int_0^t \mathrm{d}\tau\Delta\hat{E}_{\mathrm{IN1}}'(\tau)\right]^2\right\rangle, \quad (53)$$

$$\mathrm{var}(N_t') \approx 4\eta A_d\langle\hat{E}_{\mathrm{OUT}}\rangle^2\left\langle\left[\int_0^t \mathrm{d}\tau\Delta\hat{E}_{\mathrm{OUT1}}'(\tau)\right]^2\right\rangle, \quad (54)$$

and

$$\begin{aligned}\mathrm{cov}(N_t, N_t') \approx 4\eta A_d\langle\hat{E}_{\mathrm{IN}}\rangle\langle\hat{E}_{\mathrm{OUT}}\rangle\left\langle\int_0^t \mathrm{d}\tau\Delta\hat{E}_{\mathrm{IN1}}'(\tau)\right. \\ \left.\times\int_0^t \mathrm{d}\tau\Delta\hat{E}_{\mathrm{OUT1}}'(\tau)\right\rangle, \end{aligned} \quad (55)$$

where

$$\Delta\hat{E}_{j1}'(t) \equiv A_d{}^{-1/2}\int_{A_d}\mathrm{d}\mathbf{x}\,\mathrm{Re}[\hat{E}_j'(\mathbf{x}, t) - \langle\hat{E}_j'(\mathbf{x}, t)\rangle] \quad (56)$$

for j = IN, OUT represents the field-quadrature fluctuations that beat with the strong mean fields to produce the photocount fluctuations. From formulas (44) and (46)–(50) we have that

$$\begin{aligned}\Delta\hat{E}_{\mathrm{IN1}}'(t) &= [\eta/(1 + \lambda\tau_d)]^{1/2}\Delta\hat{E}_{S1}(t) + [\eta\lambda\tau_d/(1 + \lambda\tau_d)]^{1/2} \\ &\quad \times \hat{E}_{\mathrm{M1}}(t) + (1 - \eta)^{1/2}\hat{E}_{\mathrm{IN}v1}(t) - (\eta P/h\nu_0) \\ &\quad \times \int \mathrm{d}\tau\Delta\hat{E}_{\mathrm{IN1}}'(\tau)h_d(t - \tau) \end{aligned} \quad (57)$$

and

$$\begin{aligned}\Delta\hat{E}_{\mathrm{OUT1}}'(t) &= -[\eta\lambda\tau_d/(1 + \lambda\tau_d)]^{1/2}\Delta\hat{E}_{S1}(t) \\ &\quad + [\eta/(1 + \lambda\tau_d)]^{1/2}\hat{E}_{M1}(t) + (1 - \eta)^{1/2} \\ &\quad \times \hat{E}_{\mathrm{OUT}v1}(t) - [\eta P/h\nu_0(\lambda\tau_d)^{1/2}] \\ &\quad \times \int \mathrm{d}\tau\Delta\hat{E}_{\mathrm{IN1}}'(\tau)h_d(t - \tau), \end{aligned} \quad (58)$$

where the time-dependent quadrature operators are obtained from the corresponding space–time-dependent field operators, as in Eq. (56). Equations (57) and (58) are linear-feedback forms that are easily solved by means of Fourier transformation, i.e., with

$$\Delta\tilde{\hat{E}}_{\mathrm{IN1}}'(f) \equiv \int dt \Delta\hat{E}_{\mathrm{IN1}}'(t)\exp(-i2\pi ft), \tag{59}$$

etc., we can show that

$$\Delta\tilde{\hat{E}}_{\mathrm{IN1}}'(f) = \frac{[\eta/(1+\lambda\tau_d)]^{1/2}[\Delta\tilde{\hat{E}}_{S1}(f) + (\lambda\tau_d)^{1/2}\tilde{\hat{E}}_{M1}(f)] + (1-\eta)^{1/2}\tilde{\hat{E}}_{\mathrm{INv1}}(f)}{1 + (\eta P/h\nu_0)H_d(f)} \tag{60}$$

and

$$\begin{aligned}\Delta\tilde{\hat{E}}_{\mathrm{OUT1}}'(f) = &-[\eta\lambda\tau_d/(1+\lambda\tau_d)]^{1/2}\Delta\tilde{\hat{E}}_{S1}(f) \\ &+ [\eta/(1+\lambda\tau_d)]^{1/2}\tilde{\hat{E}}_{M1}(f) \\ &+ (1-\eta)^{1/2}\tilde{\hat{E}}_{\mathrm{OUTv1}}(f) \\ &- [\eta P/h\nu_0(\lambda\tau_d)^{1/2}]\Delta\tilde{\hat{E}}_{\mathrm{IN1}}(f)H_d(f),\end{aligned} \tag{61}$$

where

$$H_d(f) = \exp(-i\pi f\tau_d)[\sin(\pi f\tau_d)]/\pi f \tag{62}$$

is the frequency response associated with the impulse response $h_d(t)$. It is now a simple matter to use the coherent-state quadrature-fluctuation statistics for $\Delta\hat{E}_{S1}$, $\hat{E}_{M1}$, $\hat{E}_{\mathrm{INv1}}$, and $\hat{E}_{\mathrm{OUTv1}}$ to prove that

$$\langle \Delta\hat{E}_{j1}'(t+\tau)\Delta\hat{E}_{k1}'(t)\rangle = \int df S_{E_{j1}'E_{k1}'}(f)\exp(i2\pi f\tau), \tag{63}$$

for j, k = IN, OUT, where the noise spectra are as follows:

$$S_{E_{\mathrm{IN1}}'E_{\mathrm{IN1}}'}(f) = 1/4|1 + (\eta P/h\nu_0)H_d(f)|^2, \tag{64}$$

$$\begin{aligned}S_{E_{\mathrm{OUT1}}'E_{\mathrm{OUT1}}'}(f) = &\ 4^{-1} + |(\eta P/h\nu_0)H_d(f)|^2/4\lambda\tau_d|1 \\ &+ (\eta P/h\nu_0)H_d(f)|^2,\end{aligned} \tag{65}$$

and

$$S_{E_{\mathrm{IN1}}'E_{\mathrm{OUT1}}'}(f) = -[\eta P/h\nu_0(\lambda\tau_d)^{1/2}]H_d^*(f)S_{E_{\mathrm{IN1}}'E_{\mathrm{IN1}}'}(f). \tag{66}$$

The behavior of the spectra [Eqs. (64) and (65)] is illustrated in Fig. 7.

To complete the second-moment analysis, we note that the high-mean-count limit requires that $t \gg \tau_d$ so that only the low-frequency behavior of the preceding noise spectra contribute to the variance and covariance in formulas (53)–(55). We then find

$$\begin{aligned}\mathrm{var}(N_t) &\approx 4[\lambda t/(1+\lambda\tau_d)]S_{E_{\mathrm{IN1}}'E_{\mathrm{IN1}}'}(0) \\ &= \lambda t/(1+\lambda\tau_d)^3 = \langle N_t\rangle/(1+\lambda\tau_d)^2,\end{aligned} \tag{67}$$

$$\begin{aligned}\mathrm{var}(N_t') &\approx 4[\lambda t\lambda\tau_d/(1+\lambda\tau_d)]S_{E_{\mathrm{OUT1}}'E_{\mathrm{OUT1}}'}(0) \\ &= [\lambda t\lambda\tau_d/(1+\lambda\tau_d)][1+\lambda\tau_d/(1+\lambda\tau_d)^2] \\ &= \langle N_t'\rangle[1+\lambda\tau_d/(1+\lambda\tau_d)^2],\end{aligned} \tag{68}$$

and

$$\begin{aligned}\mathrm{cov}(N_t, N_t') &\approx 4[\lambda t(\lambda\tau_d)^{1/2}/(1+\lambda\tau_d)]S_{E_{\mathrm{IN1}}'E_{\mathrm{OUT1}}'}(0) \\ &= \lambda t\lambda\tau_d/(1+\lambda\tau_d)^3.\end{aligned} \tag{69}$$

Formula (67) reproduces the semiclassical dead-time result [Eq. (34)]; it is sub-Poisson for all $\lambda\tau_d$ values. Formulas (68) and (69) are novel.[38] In dead-time parlance, formula (68) is the variance of the counts missed because of dead time; it is super-Poisson for all $\lambda\tau_d$ values. As a consistency check on formulas (68) and (69), we note that they imply that

$$\mathrm{var}(N_t + N_t') = \mathrm{var}(N_t) + \mathrm{var}(N_t') + 2\,\mathrm{cov}(N_t, N_t') = \lambda t, \tag{70}$$

in agreement with the previously stated physical argument that $N_t + N_t'$ must be a Poisson process of rate λ. Moreover, even though we gave a quantum version of that argument, $N_t + N_t'$ being a Poisson process of rate λ also follows from the semiclassical shot-noise descriptions.[39]

Before proceeding to the NLFP case, some elaboration on what has just been shown is in order. Both the semiclassical and the quantum theories of photodetection predict the same mean and variance for the DTMPP in-loop count record N_t. This agreement is not coincidental. The semiclassical statistics will be the same as those of the quantum theory in any closed-loop photodetection arrangement in which breaking the feedback loop leaves the photodetector

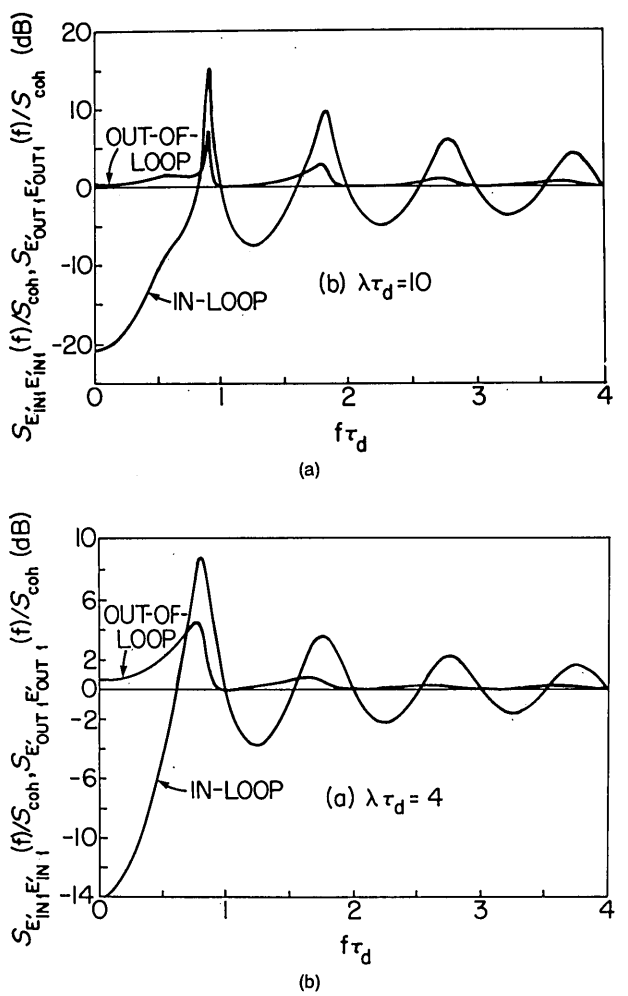

Fig. 7. Normalized first-quadrature noise spectra $S_{E_{\mathrm{IN1}}'E_{\mathrm{IN1}}'}(f)/S_{\mathrm{coh}}$ and $S_{E_{\mathrm{OUT1}}'E_{\mathrm{OUT1}}'}(f)/S_{\mathrm{coh}}$ (in decibels) versus normalized frequency $f\tau_d$ from the DTMPP quantum analysis. $S_{\mathrm{coh}} = \frac{1}{4}$ is the coherent-state noise spectrum. (a) $\lambda\tau_d = 4$ and (b) $\lambda\tau_d = 10$.

illuminated by a classical state [in the usual open-loop sense, cf. Eq. (23)]. In other words, despite our use of operator representations for photocurrents, the actual quantum measurement occurs at the photodetector, and the feedback path is entirely classical. Thus, if the open-loop illumination does not require the use of quantum photodetection theory, then neither does the closed-loop illumination. Conversely, if the open-loop illumination is nonclassical, then the closed-loop behavior must be analyzed quantum mechanically. For example, suppose the $\hat{E}_S$ field in the DTMPP analysis is in a broadband squeezed state with the mean field given by Eq. (35) and low-frequency first-quadrature noise squeezing[40]

$$S_{E_{S1}E_{S1}}(f) \approx \gamma/4 \qquad \text{for } |f| \leq 1/\pi\tau_d, \tag{71}$$

with $\gamma \ll 1$. Equations (67) and (68) then become

$$\text{var}(N_t) \approx \langle N_t \rangle [1 - (1-\gamma)\eta/(1+\lambda\tau_d)]/(1+\lambda\tau_d)^2 \tag{72}$$

and

$$\text{var}(N_t') \approx \langle N_t' \rangle [1 + \lambda\tau_d/(1+\lambda\tau_d)^2 - \eta\lambda\tau_d(1-\gamma) \times (2+\lambda\tau_d)^2/(1+\lambda\tau_d)^3], \tag{73}$$

respectively. For $\lambda\tau_d \gg 1$ and $\eta \approx 1$, the out-of-loop photocounts N_t' are strongly sub-Poisson, a result that cannot be obtained semiclassically as N_t' is an open-loop count record.

B. Negative-Linear-Feedback Process

Our second example of closed-loop photodetection is the NLFP whose semiclassical construct is sketched in Fig. 8. In this arrangement, the in-loop photocurrent i_t drives an optical intensity modulator through a causal linear time-invariant filter of impulse response $h_f(t)$. As a result, for nonrandom input light of constant power P_0, the optical power emerging from the intensity modulator obeys the negative-feedback law

$$P_t(\{i_\tau\colon\ \tau < t\}) = P_0 - (P_1/q)\int_{-\infty}^{t} i_\tau h_f(t-\tau)\mathrm{d}\tau, \tag{74}$$

conditioned on knowledge of the in-loop event history. To ensure that Eq. (74) represents negative feedback, it is sufficient to require $P_1 \geq 0$ and $h_f(t) \geq 0$ for all t.[41] Because $P_t(\{i_\tau\colon \tau < t\}) \geq 0$ must prevail under all circumstances, Eq. (74) should be viewed as an approximation, even under the preceding negative-feedback conditions, whose validity requires that the feedback term on the right-hand side in Eq. (74) be smaller than the input power with overwhelming probability. It is interesting to note that the DTMPP is a NLFP with $h_f(t) = h_d(t)$ and $P_1 = P_0$. For the DTMPP no probabilistic restriction was needed to guarantee that $P_t \geq 0$, but stochastic linearization expedited the analysis. In what follows, we treat the NLFP, with an arbitrary negative feedback $h_f(t)$, using a similar stochastic linearization both to ensure $P_t \geq 0$ and to effect steady-state statistical analysis. Moreover, to make explicit the behavior of our general results, we use the single-pole filter

$$h_f(t) = \begin{cases} \exp(-t/\tau_f) & t > 0 \\ 0 & \text{otherwise} \end{cases} \tag{75}$$

as a running example. We treat the first- and second-moment statistics of the in-loop photocurrent i_t and the out-of-loop photocurrent i_t' using the semiclassical and quantum theories, beginning with the former.

We have from stationary-process MCR theory [see Eqs. (13) and (7)] that

$$\langle i \rangle = q w_1 = q \lim_{\Delta t \to 0} [\Delta t^{-1} \Pr(\Delta N_t = 1)] \tag{76}$$

and likewise

$$\langle i' \rangle = q \lim_{\Delta t \to 0} [\Delta t^{-1} \Pr(\Delta N_t' = 1)]. \tag{77}$$

If we employ iterated expectation on the right-hand side in Eq. (76), using the incremental SEPP description [Eqs. (3)–(5)] with $\mu_t = \eta\epsilon P_t/h\nu_0$ for ϵ the beam splitter's intensity transmission, we find that

$$\langle i \rangle = q\eta\epsilon \langle P_t \rangle /h\nu_0 = (q\eta\epsilon/h\nu_0)[P_0 - (P_1/q)\langle i \rangle H_f(0)], \tag{78}$$

where $H_f(f)$ is the frequency response associated with $h_f(t)$. Equation (78) can be solved for $\langle i \rangle$, yielding

$$\langle i \rangle = (q\eta\epsilon P_0/h\nu_0)/[1 + (\eta\epsilon P_1/h\nu_0)H_f(0)], \tag{79}$$

which reduces to

$$\langle i \rangle = (q\eta\epsilon P_0/h\nu_0)/(1 + \eta\epsilon P_1\tau_f/h\nu_0) \tag{80}$$

for the single-pole filter example. In a similar manner we can show that

$$\langle i' \rangle = q\eta(1-\epsilon)\langle P_t \rangle /h\nu_0. \tag{81}$$

Somewhat greater effort is required to deduce the second moments, which are dealt with below.

From Eqs. (14) and (7) of the stationary-process MCR theory, it follows that the in-loop photocurrent covariance is of the form

$$\text{cov}(i_{t+\tau}, i_t) = q\langle i \rangle \delta(\tau) + \mathcal{K}_{ii}(\tau), \tag{82}$$

with a symmetric nonsingular component given by

$$\mathcal{K}_{ii}(\tau) = q^2 \lim_{\Delta t \to 0} \{(\Delta t)^{-2} \Pr[\Delta N_{t+\tau}\Delta N_t = 1]\} - \langle i \rangle^2 \tag{83}$$

for $\tau \neq 0$. By iterated expectation and the incremental SEPP description, we obtain

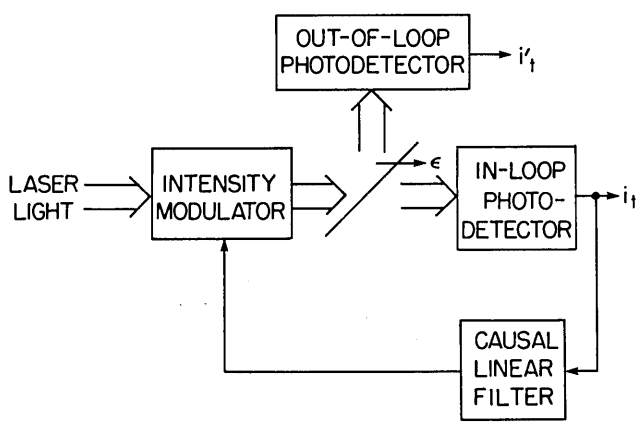

Fig. 8. Semiclassical-photodetection configuration for the NLFP experiments carried out by Machida and Yamamoto[20] and Yamamoto *et al.*[21]

$$\mathcal{K}_{ii}(\tau) = (q\eta\epsilon/h\nu_0)\langle P_{t+\tau}i_t\rangle - \langle i\rangle^2 \qquad \text{for } \tau > 0, \tag{84}$$

which is easily reduced to the following Wiener–Hopf equation[42]:

$$\mathcal{K}_{ii}(\tau) = -(\eta\epsilon P_1/h\nu_0)\left[q\langle i\rangle h_f(\tau) + \int_0^\infty \mathcal{K}_{ii}(\tau - s)h_f(s)\mathrm{d}s\right] \tag{85}$$

for $\tau > 0$. With the same approach, we find that the out-of-loop photocurrent covariance is

$$\mathrm{cov}(i_{t+\tau}', i_t') = q\langle i'\rangle\delta(\tau) + \mathcal{K}_{i'i'}(\tau), \tag{86}$$

where the symmetric nonsingular component $\mathcal{K}_{i'i'}$ satisfies

$$\mathcal{K}_{i'i'}(\tau) = -[\eta(1-\epsilon)P_1/h\nu_0]\int_0^\infty \mathrm{cov}(i_{t+\tau-s}, i_t')h_f(s)\mathrm{d}s \tag{87}$$

for $\tau > 0$ and the nonsingular cross covariance between the in-loop and out-of-loop photocurrents satisfies

$$\mathrm{cov}(i_{t+\tau}, i_t') = \begin{cases}[(1-\epsilon)/\epsilon]\mathcal{K}_{ii}(\tau) & \text{for } \tau < 0\\ [\epsilon/(1-\epsilon)]\mathcal{K}_{i'i'}(\tau) & \text{for } \tau > 0\end{cases}. \tag{88}$$

The solutions to Eqs. (82)–(88) are not difficult to obtain and are best expressed in terms of the noise spectral densities associated with the photocurrent covariances and the noise cross-spectral density associated with the photocurrent cross covariance. The results are[43]

$$S_{ii}(f) = q\langle i\rangle/|1 + (\eta\epsilon P_1/h\nu_0)H_f(f)|^2, \tag{89}$$

$$S_{i'i'}(f) = q\langle i'\rangle\{1 + |\eta[\epsilon(1-\epsilon)]^{1/2}P_1H_f(f)/h\nu_0|^2/|1 + (\eta\epsilon P_1/h\nu_0)H_f(f)|^2\}, \tag{90}$$

and

$$S_{ii'}(f) = -q[\langle i\rangle\langle i'\rangle\epsilon(1-\epsilon)]^{1/2}[\eta P_1H_f^*(f)/h\nu_0]/|1 + (\eta\epsilon P_1/h\nu_0)H_f(f)|^2. \tag{91}$$

From these spectra, it follows that the normalized differenced photocurrent, $i_-(t) \equiv [(1-\epsilon)/\epsilon]^{1/2}i_t - [\epsilon/(1-\epsilon)]^{1/2}\,i_t'$, has a white-noise spectrum equal to the sum of the i_t and i_t' shot-noise levels

$$S_{i_-i_-}(f) = q[\langle i\rangle + \langle i'\rangle], \tag{92}$$

whereas the in-loop photocurrent has a sub-shot-noise spectrum at frequencies for which $|1 + (\eta\epsilon P_1/h\nu_0)H_f(f)| > 1$, and the out-of-loop photocurrent has a super-shot-noise spectrum at all frequencies. These characteristics are illustrated in Fig. 9, where we have plotted the normalized spectra $S_{ii}(f)/q\langle i\rangle$ and $S_{i'i'}(f)/q\langle i'\rangle$ for the single-pole filter example with $\epsilon = \frac{1}{2}$.

The preceding results bear on the recent experiments of Machida and Yamamoto[20] and Yamamoto *et al.*[21] These authors used a GaAs/AlGaAs injection laser diode to generate light and a Si P–I–N photodiode to detect it. Negative electrical feedback from the detector was provided to the current driving the laser diode. Operation in a configuration analogous to Fig. 8, with $\epsilon = \frac{1}{2}$, then led to a sub-shot-noise in-loop photocurrent spectrum, a super-shot-noise out-of-loop photocurrent spectrum, and a sum of shot-noises difference-current spectrum. Yamamoto *et al.*[21] gave a quantum treatment of the laser-photodetector-feedback apparatus that predicts these results. Later, Haus and Yamamoto,[44] in their analysis of feedback-generated squeezed states, showed there was an equivalent semiclassical formulation for the experiments reported in Refs. 20 and 21. Our preliminary semiclassical work appeared in Ref. 16; it separates the feedback loop from the laser source by employing an external intensity modulator, as shown here in Fig. 8. In what follows we present our quantum analysis of the i_t and i_t' statistics. After showing how Eqs. (80), (81), and (89)–(91) are reproduced quantum mechanically, we contrast their semiclassical and quantum interpretations.

Our quantum treatment of the NLFP parallels our quantum DTMPP development. It is based on the arrangement shown in Fig. 10, in which a coherent-state signal field $\hat{E}_S(\mathbf{x}, t)$ with mean given by Eq. (35) illuminates in-loop and out-of-loop photodetectors through a lossless modulated beam splitter and a lossless ordinary beam splitter. The modulated beam splitter yields both an in-loop field

$$\hat{E}(\mathbf{x}, t) = [T(t)]^{1/2}\hat{E}_S(\mathbf{x}, t) + [1 - T(t)]^{1/2}\hat{E}_M(\mathbf{x}, t), \tag{93}$$

in terms of the beam-splitter transmission

$$T(t) = (P_0/P) - (P_1/Pq)\int i_\tau h_f(t-\tau)\mathrm{d}\tau, \tag{94}$$

and a vacuum-state field operator $\hat{E}_M(\mathbf{x}, t)$. The in-loop

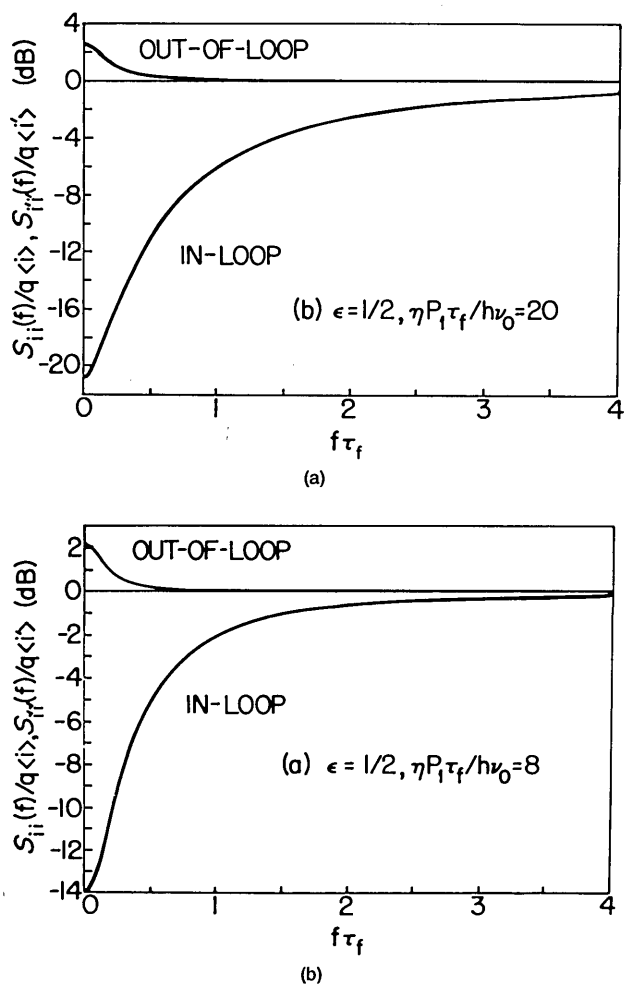

Fig. 9. Normalized NLFP photocurrent spectra $S_{ii}(f)/q\langle i\rangle$ and $S_{i'i'}(f)/q\langle i'\rangle$ (in decibels) versus normalized frequency $f\tau_f$ for single-pole filter example. (a) $\epsilon = \frac{1}{2}$, $\eta P_1\tau_f/h\nu_0 = 8$; (b) $\epsilon = \frac{1}{2}$, $\eta P_1\tau_f/h\nu_0 = 20$.

and out-of-loop photocurrents correspond to the operator measurements, Eqs. (40) and (41), respectively, where the effective fields $\hat{E}_{\mathrm{IN}'}$ and $\hat{E}_{\mathrm{OUT}'}$ are obtained from Eq. (42) and the ordinary beam-splitter relations

$$\hat{E}_{\mathrm{IN}}(\mathbf{x}, t) = \epsilon^{1/2}\hat{E}(\mathbf{x}, t) + (1-\epsilon)^{1/2}\hat{E}_B(\mathbf{x}, t), \tag{95}$$

$$\hat{E}_{\mathrm{OUT}}(\mathbf{x}, t) = -(1-\epsilon)^{1/2}\hat{E}(\mathbf{x}, t) + \epsilon^{1/2}\hat{E}_B(\mathbf{x}, t), \tag{96}$$

where yet another vacuum-state field operator $\hat{E}_B$ is introduced. The introduction of the vacuum-state fields $\{\hat{E}_M, \hat{E}_B\}$ comes from the necessity of preserving open-loop commutator brackets after propagation through the beam splitters when the feedback path is absent. The vacuum-state fields $\{\hat{E}_{\mathrm{IN}v}, \hat{E}_{\mathrm{OUT}v}\}$ are required for lossy ($\eta < 1$) detectors because of the fluctuation–dissipation theorem, which, loosely stated, implies that quantum noise is injected whenever loss is encountered, again because of commutator conservation.[45] An investigation of closed-loop NLFP commutator behavior will be of interest below, and toward that end we introduce here the auxiliary output-field relation for the modulated beam splitter:

$$\hat{E}_{\mathrm{AUX}}(\mathbf{x}, t) = -[1-T(t)]^{1/2}\hat{E}_S(\mathbf{x}, t) + [T(t)]^{1/2}\hat{E}_M(\mathbf{x}, t). \tag{97}$$

At this juncture, the analysis can proceed rapidly. Invoking an operator linearization of Eqs. (93)–(96), as was done for the DTMPP, and introducing time-dependent quadrature operators, in a manner similar to Eq. (56), we find that

$$\langle \hat{E}_{\mathrm{IN}'} \rangle = \{\eta\epsilon P_0/h\nu_0 A_d[1 + (\eta\epsilon P_1/h\nu_0)H_f(0)]\}^{1/2}, \tag{98}$$

$$\langle \hat{E}_{\mathrm{OUT}'} \rangle = -[(1-\epsilon)/\epsilon]^{1/2}\langle \hat{E}_{\mathrm{IN}'} \rangle, \tag{99}$$

$$\begin{aligned}\Delta\hat{E}_{\mathrm{IN}j}'(t) = {} & [\eta\epsilon\langle T\rangle]^{1/2}\Delta\hat{E}_{Sj}(t) + [\eta\epsilon(1-\langle T\rangle)]^{1/2} \\ & \times \hat{E}_{Mj}(t) + [\eta(1-\epsilon)]^{1/2}\hat{E}_{Bj}(t) \\ & + (1-\eta)^{1/2}\hat{E}_{\mathrm{IN}vj}(t) - \delta_{1j}(\eta\epsilon P_1/h\nu_0) \\ & \times \int \Delta\hat{E}_{\mathrm{IN1}}'(\tau)h_f(t-\tau)\mathrm{d}\tau,\end{aligned} \tag{100}$$

and

$$\begin{aligned}\Delta\hat{E}_{\mathrm{OUT}j}'(t) = {} & -[\eta(1-\epsilon)\langle T\rangle]^{1/2}\Delta\hat{E}_{Sj}(t) - [\eta(1-\epsilon) \\ & \times (1-\langle T\rangle)]^{1/2}\hat{E}_{Mj}(t) + (\eta\epsilon)^{1/2}\hat{E}_{Bj}(t) \\ & + (1-\eta)^{1/2}\hat{E}_{\mathrm{OUT}vj}(t) + \delta_{1j}[\epsilon(1-\epsilon)]^{1/2} \\ & \times (\eta P_1/h\nu_0)\int \Delta\hat{E}_{\mathrm{IN1}}'(\tau)h_f(t-\tau).\end{aligned} \tag{101}$$

In Eqs. (100) and (101)

$$\langle T\rangle = (P_0/P)/[1 + (\eta\epsilon P_1/h\nu_0)H_f(0)] \tag{102}$$

is the average modulated beam-splitter transmission, and $j = 1, 2$ denote the real and imaginary quadratures, respectively [cf. Eq. (56)]. Note that the feedback affects only the real-quadrature fluctuations, i.e., those in phase with the mean field.

The first and second moments of i_t and i_t' are easily obtained from Eqs. (98)–(102). With the linearized formulation we know that

$$\begin{aligned}\langle i_t\rangle &= qA_d(\langle \hat{E}_{\mathrm{IN}'}\rangle)^2 \\ &= (q\eta\epsilon P_0/h\nu_0)/[1 + (\eta\epsilon P_1/h\nu_0)H_f(0)]\end{aligned} \tag{103}$$

and

$$\begin{aligned}\langle i_t'\rangle &= qA_d(\langle \hat{E}_{\mathrm{OUT}'}\rangle)^2 \\ &= [q\eta(1-\epsilon)P_0/h\nu_0]/[1 + (\eta\epsilon P_1/h\nu_0)H_f(0)],\end{aligned} \tag{104}$$

in agreement with the semiclassical results [Eqs. (79) and (81)]. Moreover, by introducing Fourier transforms as in Eq. (59), we can solve the first-quadrature relations in Eqs. (100) and (101), with the following results:

$$\Delta\tilde{\hat{E}}_{\mathrm{IN1}}'(f) = \frac{[\eta\epsilon\langle T\rangle]^{1/2}\Delta\tilde{\hat{E}}_{S1}(f) + [\eta\epsilon(1-\langle T\rangle)]^{1/2}\tilde{\hat{E}}_{M1}(f) + [\eta(1-\epsilon)]^{1/2}\tilde{\hat{E}}_{B1}(f) + (1-\eta)^{1/2}\tilde{\hat{E}}_{\mathrm{IN}v1}(f)}{1 + (\eta\epsilon P_1/h\nu_0)H_f(f)} \tag{105}$$

and

$$\begin{aligned}\Delta\tilde{\hat{E}}_{\mathrm{OUT1}}'(f) = {} & -[\eta(1-\epsilon)\langle T\rangle]^{1/2}\Delta\tilde{\hat{E}}_{S1}(f) \\ & - [\eta(1-\epsilon)(1-\langle T\rangle)]^{1/2}\tilde{\hat{E}}_{M1}(f) + (\eta\epsilon)^{1/2} \\ & \times \tilde{\hat{E}}_{B1}(f) \\ & + (1-\eta)^{1/2}\tilde{\hat{E}}_{\mathrm{OUT}v1}(f) + [\epsilon(1-\epsilon)]^{1/2} \\ & \times (\eta P_1/h\nu_0)\Delta\tilde{\hat{E}}_{\mathrm{IN1}}'(f)H_f(f).\end{aligned} \tag{106}$$

From these solutions we then obtain the quadrature noise spectra [see Eq. (63)]

$$S_{E_{\mathrm{IN1}}'E_{\mathrm{IN1}}'}(f) = 1/4|1 + (\eta\epsilon P_1/h\nu_0)H_f(f)|^2, \tag{107}$$

$$\begin{aligned}S_{E_{\mathrm{OUT1}}'E_{\mathrm{OUT1}}'}(f) = {} & 4^{-1} + \epsilon(1-\epsilon)|(\eta P_1/h\nu_0)H_f(f)|^2/4|1 \\ & + (\eta\epsilon P_1/h\nu_0)H_f(f)|^2,\end{aligned} \tag{108}$$

and

$$S_{E_{\mathrm{IN1}}'E_{\mathrm{OUT1}}'}(f) = [\epsilon(1-\epsilon)]^{1/2}(\eta P_1/h\nu_0)\, H_f^*(f)S_{E_{\mathrm{IN1}}'E_{\mathrm{IN1}}'}(f). \tag{109}$$

The quantum second-moment derivations are completed by substituting Eqs. (107)–(109) into the relations

$$S_{ii}(f) = 4q\langle i\rangle S_{E_{\mathrm{IN1}}'E_{\mathrm{IN1}}'}(f), \tag{110}$$

$$S_{i'i'}(f) = 4q\langle i'\rangle S_{E_{\mathrm{OUT1}}'E_{\mathrm{OUT1}}'}(f), \tag{111}$$

and

$$S_{ii'}(f) = -4q[\langle i\rangle\langle i'\rangle]^{1/2}S_{E_{\mathrm{IN1}}'E_{\mathrm{OUT1}}'}(f), \tag{112}$$

which follow from linearization [cf. formulas (53)–(55)]. The photocurrent spectra and cross spectrum thus obtained coincide with the semiclassical formulas [Eqs. (89)–(91)].

Even though the semiclassical and quantum theories for the NLFP yield identical statistics, their physical interpretations are quite different. Consider the semiclassical Fig. 8

system: When the feedback path to the intensity modulator is broken, i_t and i_t' are statistically independent stationary shot-noise processes arising from the independent random atomic excitations occurring in the two detectors under steady classical illumination. Closing the loop reduces the i_t noise level at frequencies within the loop bandwidth as in any negative-feedback stabilization scheme.[46] This in-loop reduction comes about by modulating the incoming light with a filtered version of the i_t shot noise. Insofar as the out-of-loop detector is concerned, said modulation constitutes an excess noise on its illumination in the usual open-loop sense. As a result, the out-of-loop photocurrent shows super-shot-noise fluctuations within the loop bandwidth. Subtracting the normalized photocurrents precisely cancels the negative-feedback noise reduction on i_t, with the random-modulation noise increase on i_t' leading to a sum-of-shot-noise spectrum for i_-.

Quantum mechanically, the feedback loop reduces the in-loop photocurrent spectrum by squeezing, within the loop bandwidth, the quadrature fluctuations of $\hat{E}_{\mathrm{IN}}(\mathbf{x}, t)$ that spatially match and are in phase with its mean field. Because of the π-rad phase shift that exists between the relative phases of the $\hat{E}$ and $\hat{E}_B$ contributions to $\hat{E}_{\mathrm{IN}}$ and $\hat{E}_{\mathrm{OUT}}$, which is a consequence of energy conservation,[47] the negative-feedback loop exacerbates the quadrature fluctuations of $\hat{E}_{\mathrm{OUT}}(\mathbf{x}, t)$ that spatially match and are in phase with its mean field.[20,21] As a result, i_t' has a super-shot-noise spectrum within the loop bandwidth. When the photocurrents are normalized and subtracted, the noise-current operator is

$$\begin{aligned}\Delta\hat{i}_-(t) \equiv \hat{i}_-(t) - \langle i_-\rangle &= [(1-\epsilon)/\epsilon]^{1/2}\Delta\hat{i}_t - [\epsilon/(1-\epsilon)]^{1/2}\Delta\hat{i}_t' \\ &= 2[q(1-\epsilon)\langle i\rangle/\epsilon]^{1/2}\Delta\hat{E}_{\mathrm{IN1}}'(t) \\ &\quad + 2[q\epsilon\langle i'\rangle/(1-\epsilon)]^{1/2}\Delta\hat{E}_{\mathrm{OUT1}}'(t) \\ &= 2[q(\langle i\rangle + \langle i'\rangle)]^{1/2}[(1-\epsilon)^{1/2}\Delta\hat{E}_{\mathrm{IN1}}'(t) \\ &\quad + \epsilon^{1/2}\Delta\hat{E}_{\mathrm{OUT1}}'(t)] \\ &= 2[q(\langle i\rangle + \langle i'\rangle)]^{1/2}\hat{E}_{B1}(t), \end{aligned} \tag{113}$$

from which the sum-of-shot-noises formula [Eq. (92)] follows immediately.[20,21]

C. Commutator Relations

Additional insight into closed-loop photodetection can be developed by examining the field commutators for the quantum NLFP configuration shown in Fig. 10. For notational compactness, we limit our discussion to spatially integrated time-dependent photon-unit field operators of the form

$$\hat{E}_S(t) = A_d^{-1/2}\int_{A_d} d\mathbf{x}\hat{E}_S(\mathbf{x}, t), \tag{114}$$

etc. Free fields of this type have the following commutators:

$$[\hat{E}_S(t), \hat{E}_S(t')] = 0 \tag{115}$$

and

$$[\hat{E}_S(t), \hat{E}_S^\dagger(t')] = \delta(t-t'), \tag{116}$$

which are equivalent to the quadrature operator commutators

$$[\hat{E}_{S1}(t), \hat{E}_{S1}(t')] = [\hat{E}_{S2}(t), \hat{E}_{S2}(t')] = 0 \tag{117}$$

and

$$[\hat{E}_{S1}(t), \hat{E}_{S2}(t')] = (i/2)\delta(t-t'). \tag{118}$$

When the field fluctuations are statistically stationary, the latter imply the Heisenberg uncertainty limit

$$S_{E_{S1}E_{S1}}(f)S_{E_{S2}E_{S2}}(f) \geq 1/16 \tag{119}$$

for the quadrature fluctuation spectra. Coherent-state light achieves the minimum-uncertainty product in expression (119) with equal noise strength in each quadrature; squeezed-state light achieves the minimum-uncertainty product in expression (119) with unequal noise strength in each quadrature.

Consider the uncertainty products, similar to the left-hand side member of expression (119), for the effective fields $\hat{E}_{\mathrm{IN}}'(t)$ and $\hat{E}_{\mathrm{OUT}}'(t)$ that drive the in-loop and out-of-loop photodetectors. We already have expressions for the first-quadrature noise spectra. The following second-quadrature noise spectra can be deduced immediately from Eqs. (100) and (101):

$$S_{E_{\mathrm{IN2}}'E_{\mathrm{IN2}}'}(f) = S_{E_{\mathrm{OUT2}}'E_{\mathrm{OUT2}}'}(f) = 1/4. \tag{120}$$

Equation (120) shows that both second-quadrature noise spectra are coherent-state results. Physically, this is so because the linearized intensity-modulation feedback does not affect the second-quadrature fluctuations as the latter are $\pi/2$ rad out of phase with the mean field. Because $S_{E_{\mathrm{OUT1}}'E_{\mathrm{OUT1}}'}(f) > 1/4$, we see that the free field $\hat{E}_{\mathrm{OUT}}'$ obeys the usual uncertainty principle [expression (119)]. On the other hand, $S_{E_{\mathrm{IN1}}'E_{\mathrm{IN1}}'}(f) < 1/4$ prevails within the loop bandwidth, so that $\hat{E}_{\mathrm{IN}}'$ violates the free-field uncertainty principle. If we use the frequency-domain result [Eq. (105)] and the corresponding formula for $\Delta\tilde{E}_{\mathrm{IN2}}'(f)$, we can easily show that

$$[\hat{E}_{\mathrm{IN}}'(t), \hat{E}_{\mathrm{IN}}'(t')] = 0 \tag{121}$$

and

$$[\hat{E}_{\mathrm{IN}}'(t), \hat{E}_{\mathrm{IN}}'^\dagger(t')] = \int df \frac{\cos[2\pi f(t-t')]}{1 + (\eta\epsilon P_1/h\nu_0)H_f(f)}, \tag{122}$$

from which the Heisenberg inequality

$$S_{E_{\mathrm{IN1}}'E_{\mathrm{IN1}}'}(f)S_{E_{\mathrm{IN2}}'E_{\mathrm{IN2}}'}(f) \geq 1/16|1 + (\eta\epsilon P_1/h\nu_0)H_f(f)|^2 \tag{123}$$

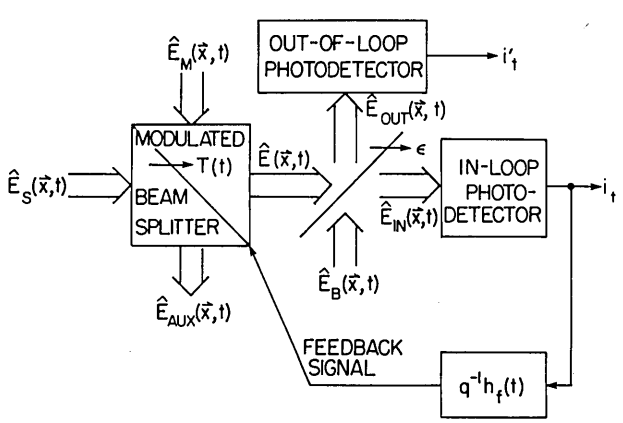

Fig. 10. Quantum-photodetection configuration for the NLFP experiments carried out by Machida and Yamamoto[20] and Yamamoto *et al.*[21]

follows readily. The in-loop effective field is operating at this uncertainty-product limit at all frequencies.

The peculiar nature of the in-loop effective-field commutator might be evidence that we have inadvertently omitted a quantum-noise contribution from our closed-loop analysis. It is germane, therefore, to examine the commutators for all the field operators involved in the arrangement shown in Fig. 10. The input operators $\{\hat{E}_S(t), \hat{E}_M(t), \hat{E}_B(t), \hat{E}_{\mathrm{IN}v}(t), \hat{E}_{\mathrm{OUT}v}(t)\}$ are commuting free-field operators obeying

$$[\hat{E}_j(t), \hat{E}_{j'}(t')] = 0 \tag{124}$$

and

$$[\hat{E}_j(t), \hat{E}_{j'}^{\dagger}(t')] = \delta_{jj'}\delta(t - t') \tag{125}$$

for $j, j' = S, M, B, \mathrm{IN}v, \mathrm{OUT}v$. Whether or not the feedback loop is closed, the open-loop output operators $\{\hat{E}_{\mathrm{AUX}}(t), \hat{E}_{\mathrm{OUT}}(t), \hat{E}_{\mathrm{OUT}'}(t)\}$ are free fields whose commutators must also satisfy Eqs. (124) and (125). That they do so can be demonstrated by means of Eqs. (93)–(97) and the linearization procedure used to derive the quadrature-noise spectra, without recourse to additional quantum-noise sources.

The in-loop field operators $\{\hat{E}(t), 4\hat{E}_{\mathrm{IN}}(t), \hat{E}_{\mathrm{IN}'}(t)\}$ are not free fields when the loop is closed, and thus they need not have the usual commutators. We have already found the $\hat{E}_{\mathrm{IN}'}(t)$ commutators. By similar calculations we obtain

$$[\hat{E}(t), \hat{E}(t')] = [\hat{E}_{\mathrm{IN}}(t), \hat{E}_{\mathrm{IN}}(t')] = 0 \tag{126}$$

and

$$[\hat{E}(t), \hat{E}^{\dagger}(t')] = [\hat{E}_{\mathrm{IN}}(t), \hat{E}_{\mathrm{IN}}{}^{\dagger}(t')] = \int \mathrm{d}f \frac{\cos[2\pi f(t - t')]}{1 + (\eta\epsilon P_1/h\nu_0)H_f(f)}, \tag{127}$$

i.e., all three in-loop fields share the same non-free-field commutator behavior.

The special character of the in-loop commutators [Eqs. (122) and (127)] is, we believe, the hallmark of the quantum closed-loop theory. It permits the in-loop photocurrent to have a sub-shot-noise spectrum, which is the semiclassical signature of the closed loop, even though all the free-field input operators are in coherent states. Indeed, were we to have $[\hat{E}_{\mathrm{IN}'}(t), \hat{E}_{\mathrm{IN}'}(t')] = 0$ and $[\hat{E}_{\mathrm{IN}'}(t), \hat{E}_{\mathrm{IN}'}{}^{\dagger}(t')] = \delta(t - t')$, with $\hat{E}_{\mathrm{IN}'}(t)$ being a linear combination of only the coherent-state field operators $[\hat{E}_S(t), \hat{E}_M(t), \hat{E}_B(t), \hat{E}_{\mathrm{IN}v}(t)]$, i_t would have to be a DSPP. Its spectrum could then never reach sub-shot-noise levels.

The preceding discussion confers a special closed-loop status on the in-loop fields $[\hat{E}(t), \hat{E}_{\mathrm{IN}}(t), \hat{E}_{\mathrm{IN}'}(t)]$ in the apparatus shown in Fig. 10. This extraordinary behavior can, nevertheless, be reconciled with the obvious facts that $\hat{E}(\mathbf{x}, t)$ represents a field in the free-space region between the modulated and ordinary beam splitters and $\hat{E}_{\mathrm{IN}}(\mathbf{x}, t)$ represents a field in the free-space region between the ordinary beam splitter and the in-loop photodetector. The key is optical propagation delay.

Our entire closed-loop analysis is of a lumped-element character, viz., no propagation delay whatsoever is included between the optical elements of the configuration of Fig. 10. It is well known that delay in a classical feedback loop can strongly affect its performance. Let us see what effects optical propagation delay has on the quantum NLFP statistics and field commutators.

Suppose that there is a τ_p-sec propagation delay between the modulated beam splitter and the ordinary beam splitter and that there is no propagation delay between the ordinary beam splitter and the in-loop and out-of-loop photodetectors. In place of Eqs. (95) and (96) we then have

$$\hat{E}_{\mathrm{IN}}(\mathbf{x}, t) = \epsilon^{1/2}\hat{E}(\mathbf{x}, t - \tau_p) + (1 - \epsilon)^{1/2}\hat{E}_B(\mathbf{x}, t), \tag{128}$$

$$\hat{E}_{\mathrm{OUT}}(\mathbf{x}, t) = -(1 - \epsilon)^{1/2}\hat{E}(\mathbf{x}, t - \tau_p) + \epsilon^{1/2}\hat{E}_B(\mathbf{x}, t). \tag{129}$$

Mimicking the development of the no-delay case, we can show that the mean photocurrents, the photocurrent spectra, and the cross spectrum all take the forms given previously with $H_f(f)$ replaced by

$$H_f'(f) \equiv \exp(-i2\pi f\tau_p)H_f(f). \tag{130}$$

Thus the physical discussion concluding Subsection 3.B continues to apply, insofar as moment behavior is concerned, subject to the impact of the delay factor on the right-hand side of Eq. (130) on the achievable noise squeezing. Said impact is illustrated in Fig. 11, where we have plotted $S_{ii}(f)/q\langle i\rangle$ for the single-pole filter example with $\epsilon = \frac{1}{2}$, $\eta P_1\tau_f/h\nu_0 = 8$, and various τ_p/τ_f values.[48]

Now let us consider the commutator behavior when optical delay is included. Here we find that the open-loop output operators $\{\hat{E}_{\mathrm{AUX}}(t), \hat{E}_{\mathrm{OUT}}(t), \hat{E}_{\mathrm{OUT}'}(t)\}$ continue to have the free-field commutators [Eqs. (124) and (125)], whereas the in-loop field operators $\{\hat{E}(t), \hat{E}_{\mathrm{IN}}(t), \hat{E}_{\mathrm{IN}'}(t)\}$ have the commutators given in Eqs. (121), (122), (126), and (127) with $H_f(f)$ replaced by $H_f'(f)$ from Eq. (130). If we now write

$$\int \mathrm{d}f \frac{\cos[2\pi f(t - t')]}{1 + (\eta\epsilon P_1/h\nu_0)H_f'(f)} = \delta(t - t') - \int \mathrm{d}f \frac{(\eta\epsilon P_1/h\nu_0)H_f'(f)\cos[2\pi f(t - t')]}{1 + (\eta\epsilon P_1/h\nu_0)H_f'(f)}, \tag{131}$$

we can use the causality of $H_f(f)$ to prove that the integral term on the right-hand side in Eq. (131) is zero for $|t - t'| < \tau_p$. Thus, for time differences smaller than the optical propagation delay, the in-loop fields have free-field commutator behavior. Physically, this means that, at any time t, the

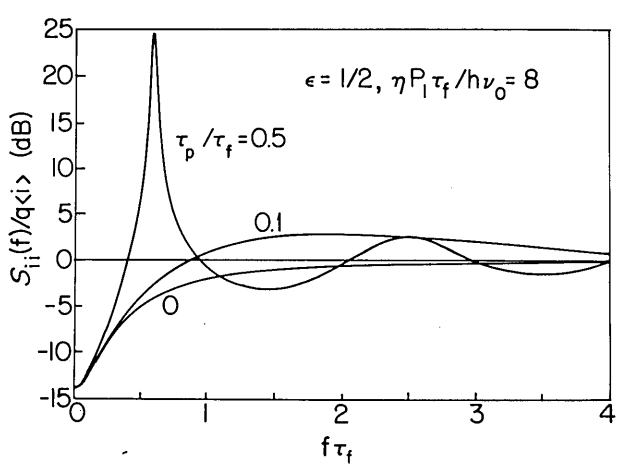

Fig. 11. Normalized NLFP in-loop photocurrent spectra $S_{ii}(f)/q\langle i\rangle$ (in decibels) versus normalized frequency $f\tau_f$ for the single-pole filter example: $\epsilon = \frac{1}{2}$; $\eta P_1\tau_f/h\nu_0 = 8$; $\tau_p/\tau_f = 0, 0.1, 0.5$.

fields present in the free-space regions between the modulated beam splitter and the ordinary beam splitter and between the ordinary beam splitter and the in-loop photodetector have no special closed-loop status. It is the feedback action over time intervals in excess of the optical propagation delay that leads to the non-free-field forms in Eqs. (122) and (127). These interpretations can be tested, conceptually, by studying the transient behavior of the in-loop photocurrent statistics when the feedback path is suddenly broken. If the field that exists at any one time between the modulated beam splitter and the in-loop detector is, in essence, a classical-state free field, then breaking the feedback path at time t_0, when the loop was in its steady state, must make $\{i_t{:}t > t_0\}$ a DSPP. The proof is as follows.

Suppose that the closed-loop system, incorporating the τ_p-sec propagation delay, is in its statistical steady state at $t = t_0$ and that the feedback path is broken by freezing the modulated beam splitter's intensity transmission for $t \geq t_0$, i.e., by forcing

$$T(t) = \langle T\rangle - 2P_1(\eta\epsilon\langle T\rangle/Ph\nu_0)^{1/2}\int \Delta\hat{E}_{\mathrm{IN}1}'(\tau)h_f'(t_0-\tau)\mathrm{d}\tau \tag{132}$$

to prevail for $t \geq t_0$, where $h_f'(t)$ is the impulse response associated with $H_f'(f)$ and $\langle T\rangle$ is still given by Eq. (102). We then find that Eq. (100) becomes

$$\begin{aligned}\Delta\hat{E}_{\mathrm{IN}j}'(t) = {}& [\eta\epsilon\langle T\rangle]^{1/2}\Delta\hat{E}_{Sj}(t-\tau_p) + [\eta\epsilon(1-\langle T\rangle)]^{1/2}\\ &\times \hat{E}_{Mj}(t-\tau_p) + [\eta(1-\epsilon)]^{1/2}\hat{E}_{Bj}(t)\\ &+ (1-\eta)^{1/2}\hat{E}_{\mathrm{IN}vj}(t) - \delta_{1j}(\eta\epsilon P_1/h\nu_0)\\ &\times \int \Delta\hat{E}_{\mathrm{IN}1}'(\tau)h_f'(t_0-\tau_p-\tau)\mathrm{d}\tau\end{aligned} \tag{133}$$

for $t \geq t_0, j = 1, 2$. Using the remarks surrounding Eq. (131), we can show from Eq. (133) that

$$[\hat{E}_{\mathrm{IN}}'(t), \hat{E}_{\mathrm{IN}}'(t')] = 0 \tag{134}$$

and

$$[\hat{E}_{\mathrm{IN}}'(t), \hat{E}_{\mathrm{IN}}'^{\dagger}(t')] = \delta(t-t') \tag{135}$$

hold for $t, t' \geq t_0$. Thus the effective photon-units field driving the in-loop photodetector for the $t \geq t_0$ transient regime has free-field commutator behavior. To prove $\{i_t{:}t > t_0\}$ is a DSPP, we need only show that $\{\hat{E}_{\mathrm{IN}}'(t){:}t > t_0\}$ is in a classical state.

Using our frequency-domain solution to the steady-state feedback form [Eq. (100) with delay included], we can show that

$$\Delta\hat{E}_{\mathrm{IN}j}'(t) = \Delta\hat{E}_{\mathrm{EFF}j}(t) - \delta_{1j}\int \Delta\hat{E}_{\mathrm{EFF}1}(\tau)h_{\mathrm{EFF}}(t_0-\tau)\mathrm{d}\tau \tag{136}$$

for $j = 1, 2$ and $t \geq t_0$, where

$$\begin{aligned}\Delta\hat{E}_{\mathrm{EFF}}(t) \equiv {}& (\eta\epsilon\langle T\rangle)^{1/2}\Delta\hat{E}_S(t-\tau_p) + [\eta\epsilon(1-\langle T\rangle)]^{1/2}\\ &\times \hat{E}_M(t-\tau_p) + [\eta(1-\epsilon)]^{1/2}\hat{E}_B(t)\\ &+ (1-\eta)^{1/2}\hat{E}_{\mathrm{IN}v}(t)\end{aligned} \tag{137}$$

is a vacuum-state field-fluctuation operator with free-field commutators for all times and $h_{\mathrm{EFF}}(t)$ is the impulse response associated with the frequency response:

$$H_{\mathrm{EFF}}(f) \equiv \frac{(\eta\epsilon P_1/h\nu_0)H_f'(f)}{1+(\eta\epsilon P_1/h\nu_0)H_f'(f)}. \tag{138}$$

So, because $h_{\mathrm{EFF}}(t)$ is zero for $t < t_p$ [cf. Eq. (131)], the integral term multiplying δ_{1j} on the right-hand side of Eq. (136) can be replaced with a classical zero-mean real-valued Gaussian random variable of variance $4^{-1}\int \mathrm{d}f|H_{\mathrm{EFF}}(f)|^2$. This demonstrates that $\Delta\hat{E}_{\mathrm{IN}}'(t)$ differs from the coherent-state field operator $\Delta\hat{E}_{\mathrm{EFF}}(t)$ on $t > t_0$ only by a c-number random variable. Hence $\{\hat{E}_{\mathrm{IN}}(t){:}t > t_0\}$ is in a classical state, and $\{i_t{:}t > t_0\}$ is a DSPP.

4. NONCLASSICAL FIELD EXTRACTION

In this our concluding section, we address the use of nonclassical light-beam correlations to extract nonclassical open-loop fields from closed-loop photodetection systems.

A. Dead-Time-Modified Poisson Process/Photon-Twins Field Extraction

Parametric downconversion and atomic-cascade emission processes both yield the photon-twin light beams that were suggested[22,23] and recently used[25] for producing open-loop sub-Poisson light by gating procedures akin to the arrangement that we have dubbed the DTMPP.[49] A basic structure for such experiments is shown in Fig. 12. The photon-twin source produces two spatially disjoint quantum fields that illuminate identical in-loop and out-of-loop photodetectors through flip-mirror arrangements driven by the in-loop photocurrent in the manner of Fig. 5. In parametric fluorescence, the photon-units fields $\hat{E}_{\mathrm{REF}}(\mathbf{x}, t)$ (center frequency ν_{REF}) and $\hat{E}_{\mathrm{SIG}}(\mathbf{x}, t)$ (center frequency ν_{SIG}) are each in classical states[50]; yet, because of energy conservation at the photon-generation level, they have perfect photon-flux correlation, namely,

$$\mathrm{var}\left\{\int_{A_d}\mathrm{d}\mathbf{x}[\hat{E}_{\mathrm{SIG}}^{\dagger}(\mathbf{x},t)\hat{E}_{\mathrm{SIG}}(\mathbf{x},t) - \hat{E}_{\mathrm{REF}}^{\dagger}(\mathbf{x},t)\hat{E}_{\mathrm{REF}}(\mathbf{x},t)]\right\} = 0. \tag{139}$$

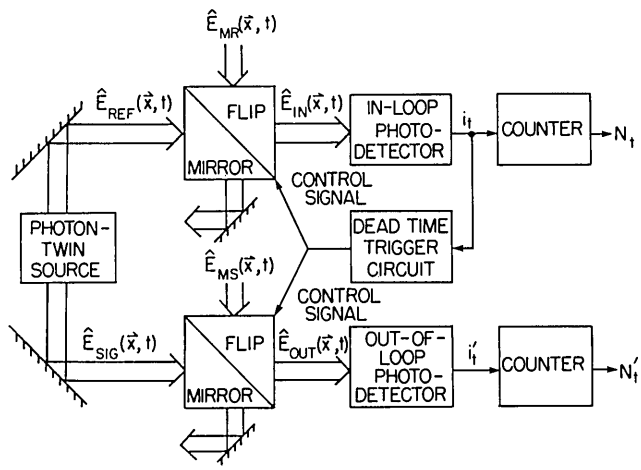

Fig. 12. Schematic for open-loop sub-Poisson beam generation by the DTMPP/photon-twins experiment. The fields $\hat{E}_{\mathrm{MR}}$ and $\hat{E}_{\mathrm{MS}}$ are quantum-mechanically independent vacuum-state photon-units operators at the reference and signal frequencies, respectively.

This correlation is exploited by using photodetections from the reference field to gate both the reference and the signal fields, resulting in a sub-Poisson out-of-loop photocount record, as will be shown below.

Let us assume that the detection area A_d comprises a sufficiently large number of spatial modes of the parametric fluorescence that the low-photon coherence condition[51] applies. We can then linearize the in-loop and out-of-loop effective photon-flux operators about their mean values and show, using techniques similar to those in Subsection 3.A, that

$$\langle N_t \rangle = \langle N_t' \rangle = \lambda t/(1 + \lambda\tau_d) \tag{140}$$

and

$$\mathrm{var}(N_t) = \langle N_t \rangle/(1 + \lambda\tau_d)^2, \tag{141}$$

$$\mathrm{var}(N_t') = \langle N_t' \rangle[1 + (1 - \eta)2\lambda\tau_d(1 + \lambda\tau_d)]/(1 + \lambda\tau_d)^2. \tag{142}$$

Here, $\lambda = \eta P_{\mathrm{REF}}/h\nu_{\mathrm{REF}} = \eta P_{\mathrm{SIG}}/h\nu_{\mathrm{SIG}}$ gives the average open-loop photoemission rate in terms of the average fluorescence power P divided by the photon energy $h\nu$ at the reference and signal frequencies, and the detector quantum efficiency η was assumed to be the same at both of these frequencies. When $\lambda\tau_d \gg 1$ the out-of-loop photocount record will be sub-Poisson with a variance limited by the imperfect effective photon-flux correlation caused by the quantum-mechanically independent $\eta < 1$ quantum noise introduced at the in-loop and out-of-loop detectors, viz.,

$$\mathrm{var}(N_t') \approx \langle N_t' \rangle 2(1 - \eta). \tag{143}$$

Production of strongly sub-Poisson open-loop light by using the DTMPP/photon-twins route will therefore require near-unity photodetector quantum efficiencies at both ν_{REF} and ν_{SIG}.

B. Negative-Linear-Feedback Process/Quantum Nondemolition Field Extraction

Yamamoto *et al.*[21] suggested that a Kerr-effect QND measurement[24] be used to extract a sub-shot-noise open-loop field from their feedback-modulated semiconductor-laser NLFP system. They also showed[21,44] how the back action of the QND measurement increases the second-quadrature (phase) noise on the extracted sub-shot-noise out-of-loop field, imparting to this field sufficient quantum noise to make its commutators take on the requisite free-field characteristics. These results can easily be reproduced in our NLFP construct, wherein the modulation is external to the laser, as sketched out below. The behavior of the semiconductor laser itself plays no part in our treatment.

Consider the NLFP/QND arrangement shown in Fig. 13. In this setup, two strong coherent-state fields, the center-frequency ν_S signal field $\hat{E}_S(\mathbf{x}, t)$, and the center-frequency ν_P probe field $\hat{E}_P(\mathbf{x}, t)$ are the principal inputs. The former transits a modulated beam splitter, in the manner of the ordinary (Fig. 10) NLFP experiment, before interacting with the probe field in the Kerr medium. The cross-phase-modulation interaction occurring over an Lm path in that medium engenders nonclassical coupling between the photon-flux density of the center-frequency ν_S signal field $\hat{E}_{\mathrm{OUT}}(\mathbf{x}, t)$ and the phase of the center-frequency ν_P probe field $\hat{E}_{\mathrm{IN}}(\mathbf{x}, t)$ that emerge. As shown by Imoto *et al.*,[24] this quantum correlation permits the photon-flux behavior of the signal field to be inferred from a homodyne-detection phase measurement on the probe field. This, in turn, permits the feedback loop to be closed by using the probe-field phase measurement instead of the signal-field direct-detection measurement.[21]

To make the preceding remarks explicit, let the input signal and probe fields have strong mean values

$$\langle \hat{E}_j(\mathbf{x}, t) \rangle = (P_j/h\nu_j A_d)^{1/2} \tag{144}$$

for $j = S, P$, where A_d will be regarded not only as a photodetector active area but also the cross section over which the Kerr interaction transpires. We neglect self-phase modulation, loss, and dispersion and assume that the phase shifts produced by cross-phase modulation are very small compared with a radian. In terms of the spatially integrated fields we then have

$$\hat{E}_{\mathrm{OUT}}(t) = \{1 + i\kappa L[(P_P/h\nu_P) + 2(P_P/h\nu_P)^{1/2} \times \Delta\hat{E}_{P1}(t - \tau_p)]\}\hat{E}(t - \tau_p) \tag{145}$$

and

$$\hat{E}_{\mathrm{IN}}(t) = \{1 + i\kappa L[\langle \hat{E} \rangle^2 A_d + 2\langle \hat{E} \rangle A_d^{1/2} \times \Delta\hat{E}_1(t - \tau_p)]\}\hat{E}_P(t - \tau_p), \tag{146}$$

where we have linearized about the strong mean fields. Here, κ is the cross-phase-modulation coupling constant, $\tau_p = L/c$ is the propagation delay, and subscript 1 denotes first field quadrature. The homodyne measurement on the in-loop probe field $\hat{E}_{\mathrm{IN}}$ is arranged to sense the second field quadrature. The operator representation for the resulting homodyne photocurrent is then[5]

$$\hat{i}_t = 2q\eta(P_{\mathrm{LO}}/h\nu_P)^{1/2}\{\kappa L(P_P/h\nu_P)^{1/2}[\langle \hat{E} \rangle^2 A_d + 2\langle \hat{E} \rangle A_d^{1/2}\Delta\hat{E}_1(t - \tau_p)] + \hat{E}_{P2}(t - \tau_p)\} + i_{\mathrm{vac}}(t), \tag{147}$$

where P_{LO} is the local-oscillator power and i_{vac} is a zero-mean white Gaussian noise process of spectrum $q^2\eta(1 - \eta)P_{\mathrm{LO}}/h\nu_P$ that represents the $\eta < 1$ quantum noise incurred in the homodyne apparatus. The feedback loop is closed by passing i_t through an amplifier of gain $K = h\nu_P/2\kappa L(P_{\mathrm{LO}}P_P)^{1/2}$

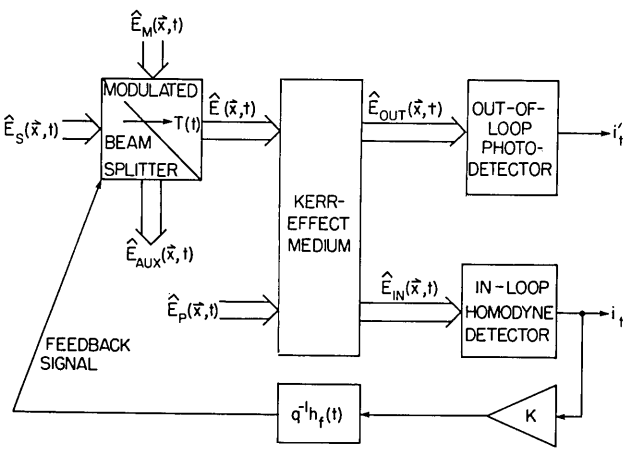

Fig. 13. Schematic for open-loop sub-shot-noise beam generation by the NLFP/QND experiment. The fields $\hat{E}_S$ and $\hat{E}_P$ are quantum-mechanically independent coherent-state photon-units operators at the signal and probe frequencies, respectively.

and the causal linear filter $q^{-1}h_f(t)$. From this point on, it is straightforward to derive the following field-quadrature and photocurrent fluctuation spectra and commutators for the out-of-loop signal field $\hat{E}_{\mathrm{OUT}}(t)$:

$$S_{E_{\mathrm{OUT1}}E_{\mathrm{OUT1}}}(f) = \frac{1 + |\eta P_1 H_f'(f)/h\nu_S|^2/4(\kappa L)^2\langle T\rangle\,\eta(P_P/h\nu_P)(P_S/h\nu_S)}{4|1 + (\eta P_1/h\nu_S)H_f'(f)|^2}, \tag{148}$$

$$S_{E_{\mathrm{OUT2}}E_{\mathrm{OUT2}}}(f) = 4^{-1}[1 + 4(\kappa L)^2\langle T\rangle\,(P_P/h\nu_P)(P_S/h\nu_S)], \tag{149}$$

$$S_{i'i'}(f) = q\langle i'\rangle\,[4\eta S_{E_{\mathrm{OUT1}}E_{\mathrm{OUT1}}}(f) + (1-\eta)], \tag{150}$$

$$[\hat{E}_{\mathrm{OUT}}(t), \hat{E}_{\mathrm{OUT}}(t')] = 0, \tag{151}$$

and

$$[\hat{E}_{\mathrm{OUT}}(t), \hat{E}_{\mathrm{OUT}}^{\dagger}(t')] = \delta(t-t'), \tag{152}$$

where $\langle T\rangle = (P_0/P_S)/[1 + (\eta P_1/h\nu_S)H_f'(0)]$ is the mean beam-splitter transmission.

We see from Eqs. (148) and (150) that when the probe power is sufficiently large the free-field output $\hat{E}_{\mathrm{OUT}}$ will be first-quadrature squeezed, within the loop bandwidth, and yield a sub-shot-noise out-of-loop photocurrent spectrum over this frequency range. We see from Eq. (149) that the second-quadrature (phase) noise on this output beam has been raised above the coherent-state level by the photon-flux (first-quadrature) probe noise introduced through the Kerr interaction [cf. Eq. (145)]. Moreover, this back action exactly reclaims the appropriate free-field commutator relations [Eqs. (151) and (152)] and therefore forces the uncertainty product obtained from Eqs. (148) and (149) to satisfy formula (119). Indeed, if we adjust the probe power P_P to minimize this uncertainty product at a selected frequency f_0, we get

$$\min_{P_P}[S_{E_{\mathrm{OUT1}}E_{\mathrm{OUT1}}}(f_0)S_{E_{\mathrm{OUT2}}E_{\mathrm{OUT2}}}(f_0)] = \frac{(1 + \eta^{1/2}P_1|H_f'(f_0)|/h\nu_S)^2}{16|1 + \eta P_1 H_f'(f_0)/h\nu_S|^2} \geq 1/16. \tag{153}$$

C. Quasi-State Synthesis

The overwhelming majority of our analysis of closed-loop photodetection has dealt with linearized feedback loops. We close by returning briefly to the general nonlinear construct. Our goal is to show how the preceding closed-loop field-extraction techniques lead to an in-principle synthesis procedure for producing an open-loop quantum light beam of arbitrary prescribed direct-detection (photocount) statistics.

Consider the open-loop photodetection of a quantized light beam using a detector of unity quantum efficiency. If the density operator (state) of this beam is totally unconstrained by previous information, then the resulting photodetection event times will comprise a similarly unconstrained SEPP. Now consider the closed-loop photodetection system in Fig. 3, where once again unity quantum efficiency is assumed. Suppose that the input light is a highly intense beam, and the optical modulator is an infinite-bandwidth electro-optic intensity modulator driven by an arbitrary causal time-varying nonlinear system run from the photocurrent. Then this photocurrent can also be an arbitrary SEPP. In other words, using the semiclassical closed-loop theory, which is valid when the input light is in a classical state, we can synthesize any SEPP by choosing the feedback function to be such that the power falling on the photodetector satisfies[52]

$$[P_t(\{\mathbf{t}_t, N_t\})]/h\nu_0 = \mu_t, \tag{154}$$

where μ_t is the conditional rate function for the desired SEPP. By this technique, we can use coherent-state light to create a closed-loop beam whose direct-detection statistics match those of any desired (classical or nonclassical state) open-loop beam. It should be clear from Subsections 4.A and 4.B and IV.B that quantum-beam correlations of either the photon-twins or Kerr-effect QND variety will permit extraction of said closed-loop field, leading to the aforestated synthesis procedure for open-loop beams of arbitrary prescribed direct-detection statistics. It should be noted, however, that open-loop direct-detection statistics do not uniquely determine the density operator of a quantum field,[5] so we cannot say that the procedure that we laid out can synthesize arbitrary prescribed field states. Such a synthesis procedure may perhaps be attainable from closed-loop heterodyne detection, inasmuch as it is known that open-loop heterodyne detection statistics do determine the density operator.[5]

ACKNOWLEDGMENTS

Two of the authors, J. H. Shapiro and P. Kumar, acknowledge valuable technical discussions with R. S. Bondurant and H. A. Haus. This research was supported in part by the National Science Foundation and the Joint Services Electronics Program.

B. E. A. Saleh is also with the Department of Electrical and Computer Engineering, University of Wisconsin, Madison, Wisconsin 53706.

REFERENCES AND NOTES

1. R. J. Glauber, Phys. Rev. **130,** 2529 (1963); **131,** 2766 (1963).
2. P. L. Kelley and W. H. Kleiner, Phys. Rev. A **136,** 316 (1964).
3. J. H. Shapiro, H. P. Yuen, and J. A. Machado Mata, IEEE Trans. Inform. Theory **IT-25,** 179 (1979).
4. H. P. Yuen and J. H. Shapiro, IEEE Trans. Inform. Theory **IT-26,** 78 (1980).
5. J. H. Shapiro, IEEE J. Quantum Electron. **QE-21,** 237 (1985).
6. L. Mandel, Proc. Phys. Soc. London **74,** 233 (1959).
7. R. M. Gagliardi and S. Karp, *Optical Communications* (Wiley, New York, 1976).
8. B. E. A. Saleh, *Photoelectron Statistics* (Springer-Verlag, Berlin, 1978).
9. H. J. Kimble, M. Dagenais, and L. Mandel, Phys. Rev. Lett. **39,** 691 (1977).
10. R. Short and L. Mandel, Phys. Rev. Lett. **51,** 384 (1983).
11. M. C. Teich and B. E. A. Saleh, J. Opt. Soc. Am. B **2,** 275 (1985).
12. R. E. Slusher, L. W. Hollberg, B. Yurke, J. C. Mertz, and J. F. Valley, Phys. Rev. Lett. **55,** 2409 (1985).
13. R. M. Shelby, M. D. Levenson, S. H. Perlmutter, R. G. DeVoe, and D. F. Walls, Phys. Rev. Lett. **57,** 691 (1986).
14. L.-A. Wu, H. J. Kimble, J. L. Hall, and H. Wu, Phys. Rev. Lett. **57,** 2520 (1986).

15. M. W. Maeda, P. Kumar, and J. H. Shapiro, Opt. Lett. **12,** 161 (1987).
16. J. H. Shapiro, M. C. Teich, B. E. A. Saleh, P. Kumar, and G. Saplakoglu, Phys. Rev. Lett. **56,** 1136 (1986).
17. D. L. Snyder, *Random Point Processes* (Wiley, New York, 1975).
18. D. R. Cox and V. Isham, *Point Processes* (Chapman and Hall, London, 1980).
19. J. G. Walker and E. Jakeman, Proc. Soc. Photo-Opt. Instrum. Eng. **492,** 274 (1985).
20. S. Machida and Y. Yamamoto, Opt. Commun. **57,** 290 (1986).
21. Y. Yamamoto, N. Imoto, and S. Machida, Phys. Rev. A **33,** 3243 (1986).
22. E. Jakeman and J. G. Walker, Opt. Commun. **55,** 219 (1985).
23. B. E. A. Saleh and M. C. Teich, Opt. Commun. **52,** 429 (1985).
24. N. Imoto, H. A. Haus, and Y. Yamamoto, Phys. Rev. A **32,** 2287 (1985).
25. J. G. Walker and E. Jakeman, Opt. Acta **32,** 1303 (1985); J. G. Rarity, P. R. Tapster, and E. Jakeman, Opt. Commun. **62,** 201 (1987).
26. Our photodetection model suppresses all noise sources, except those fundamental to the optical-to-electrical conversion process. We employ the photon-flux-driven description of this conversion, although our analysis is not highly sensitive to this assumption. See Ref. 5 for further elaboration on these points.
27. In effect, we are saying that the optical-to-electrical conversion process has infinite bandwidth. So long as the actual photodetector bandwidth greatly exceeds that of the loop filters employed in the analysis of Section 3, this assumption is warranted.
28. Throughout what follows we alternate between considering statistics for N_t and i_t, choosing whichever viewpoint best lends itself to the argument at hand. It follows from Eq. (1) that no loss of generality ensues from this vacillation.
29. The photon-units field operator has the commutators $[\hat{E}(\mathbf{x}, t), \hat{E}(\mathbf{x}', t')] = 0$, $[\hat{E}(\mathbf{x}, t), \hat{E}^\dagger(\mathbf{x}', t')] = \delta(\mathbf{x} - \mathbf{x}')\,\delta(t - t')$ in the open-loop (free-field) configuration. Closed-loop commutator behavior is treated in Section 3.
30. M. Sargent, M. O. Scully, and W. E. Lamb, *Laser Physics* (Addison-Wesley, Reading, Mass., 1974), pp. 301–303.
31. M. C. Teich and B. E. A. Saleh, Opt. Lett. **7,** 365 (1982); J. Peřina, B. E. A. Saleh, and M. C. Teich, Opt. Commun. **48,** 212 (1983).
32. M. C. Teich, B. E. A. Saleh, and J. Peřina, J. Opt. Soc. Am. B **1,** 366 (1984).
33. It follows from Theorem 1 of Ref. 4 that the statistics of the classical photocurrent i_t coincide with those of the quantum measurement $\hat{i}_t$ over any time interval. Thus, in photocurrent signal-processing calculations we may use the classical and quantum descriptors interchangeably, as demonstrated for open-loop coherent detection in Refs. 4 and 5. This same duality of viewpoint will be employed below for closed-loop configurations.
34. L. M. Ricciardi and F. Esposito, Kybernetik **3,** 148 (1966).
35. B. I. Cantor and M. C. Teich, J. Opt. Soc. Am. **65,** 786 (1975).
36. M. C. Teich and G. Vannucci, J. Opt. Soc. Am. **68,** 1338 (1978).
37. This is a stochastic linearization, i.e., the standard deviations of the filtered operator-valued fluctuations are taken to be small compared with their associated mean values. Strictly speaking, this linearization should be performed on the space–time integrated-field operators used below in formulas (53)–(55). It is simpler, however, to do the linearization at the outset, as the same final results are obtained.
38. J. W. Müller, International Bureau of Weights and Measures, Pavillon de Breteuil, Sevrès, France (personal communication).
39. If we tie the two photodetectors together so that i_t drives the flip mirror but $i_t + i_t'$ drives the counter circuit, it is clear that $i_t + i_t''$ is equivalent to the photocurrent from a single photodetector under constant illumination at power P. The associated counting process for that equivalent detector in semiclassical theory is a Poisson process of rate λ.
40. The noise-reduction parameter γ cannot be made arbitrarily small at fixed mean field without violating the high-mean-count linearization assumption.
41. Negative feedback certainly prevails at all times when $P_1 h_f(t) \geq 0$ for all t, but this condition is overly restrictive. A weaker sufficient condition for the validity of the NLFP results that we develop is that the closed loop be stable, i.e., $|1 + (\eta\epsilon P_1/h\nu_0)H_f(f)| > 0$ for all f, where H_f is the frequency response associated with h_f.
42. H. L. Van Trees, *Detection, Estimation, and Modulation Theory, Part I* (Wiley, New York, 1968), Chap. 6.
43. That Eqs. (89)–(91) satisfy Eqs. (82)–(88) can be verified by substitution, using the causality of $H_f(f)$ and the associated feedback form $1/[1 + (\eta\epsilon P_1/h\nu_0)H_f(f)]$.
44. H. A. Haus and Y. Yamamoto, Phys. Rev. A **34,** 270 (1986).
45. W. H. Louisell, *Quantum Statistical Properties of Radiation* (Wiley, New York, 1973).
46. In particular, the i_t noise level is reduced at all frequencies for which the feedback is negative, viz., $|1 + (\eta\epsilon P_1/h\nu_0)H_f(f)| > 1$. Note that positive feedback, i.e., $|1 + (\eta\epsilon P_1/h\nu_0)H_f(f)| < 1$, can prevail at some frequencies, even though $P_1 h_f(t) \geq 0$ for all t; see Fig. 7.
47. B. L. Schumaker, Opt. Lett. **9,** 189 (1984).
48. By using $H_f'(f) = \exp[-i2\pi f(\tau_p + \tau_e)]H_f(f)$ in Eq. (130) we can account for any electrical delay τ_e in the feedback path. Figure 11 can then be viewed as a function of the normalized total delay encountered when the loop is closed around the modulated beam splitter.
49. E. Jakeman and J. H. Jefferson, Opt. Acta **33,** 557 (1986).
50. The individual classical-state character of $\hat{E}_{\mathrm{REF}}$ and $\hat{E}_{\mathrm{SIG}}$ is easily demonstrated for a parametric downconverter in which the pump field and the nonlinear medium are treated classically, see, e.g., W. H. Louisell, *Radiation and Noise in Quantum Electronics* (McGraw-Hill, New York, 1964), pp. 274–278.
51. R. S. Kennedy, Proc. IEEE **58,** 1651 (1970).
52. Because μ_t depends only on the photocount record up to time t, Eq. (154) can be achieved with a causal feedback system. However, the conditional rate can diverge, see, e.g., the number-state example in Ref. 3. Thus, because our intensity modulator can act only as a variable attenuator, we must have available a very intense input beam. Furthermore, because μ_t undergoes, in general, abrupt transitions as each photodetection event occurs, the feedback system and the intensity modulator must possess enormous (near-infinite) bandwidths. While these considerations may detract from the practicality of achieving Eq. (154), they do not detract from the 1:1 relationship that Eq. (154) establishes between open-loop quantum photodetection and closed-loop semiclassical photodetection.

(*see overleaf*)

G. Saplakoglu

G. Saplakoglu was born in Ankara, Turkey, on May 3, 1961. He received the B.S. and M.S. degrees in electrical engineering from the Middle East Technical University, Ankara, Turkey, in 1982 and 1984, respectively. He was awarded a NATO science scholarship in 1984. Since September 1984 he has been working toward a Ph.D. degree in electrical engineering at the Massachusetts Institute of Technology. His research interests lie in the areas of communication theory, optical communications, and quantum optics.

S.-T. Ho

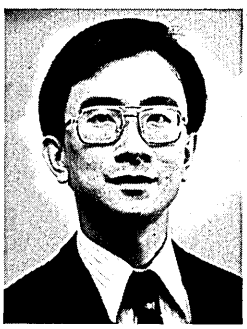

S.-T. Ho was born in Singapore on May 15, 1958. After Pre-University, he served two and a half years' National Service as an infantry officer. He received the S.B. degrees in physics and electrical engineering in 1984, the S.M. degree in electrical engineering and computer science in 1984, and the E.E. degree in 1986, all from the Massachusetts Institute of Technology. He was affiliated with Northrop Corporation, Norwood, Massachusetts, as a student intern from 1981 to 1983. He is now working toward the Ph.D. degree in electrical engineering at MIT. He has published several papers on reducing frequency noise in semiconductor lasers and on the quantum theory of atom–field interactions. He was awarded the Newport Research Award by the Optical Society of America in 1986. His current interest is in the generation of the squeezed states of light. Mr. Ho is a member of Phi Beta Kappa, Sigma Xi, Sigma Pi Sigma, and Tau Beta Pi.

Bahaa E. A. Saleh

Bahaa E. A. Saleh received the B.S. degree from Cairo University in 1966 and the Ph.D. degree from Johns Hopkins University in 1971, both in electrical engineering. From 1971 to 1974 he was an assistant professor at the University of Santa Catarina, Brazil. Thereafter, he joined the Max-Planck Institute, Göttingen, Federal Republic of Germany, where he was involved in research in laser light scattering and photon-correlation spectroscopy. He is currently professor of electrical and computer engineering at the University of Wisconsin, Madison, where he has been since 1977. He held visiting appointments at the University of Kuwait in 1976, the School of Optometry of the University of California at Berkeley in 1977, and the Columbia Radiation Laboratory of Columbia University, New York, in 1983. He is currently involved in research in image processing, optical information processing, statistical optics, quantum optics, optical communication, and vision. He is the author of *Photoelectron Statistics* (Springer, New York, 1978) and a coeditor of *Transformations in Optical Signal Processing* (Society of Photo-Optical, 1981). From 1980 to 1983 he was an associate editor of the *Journal of the Optical Society of America*, and since 1983 he has been a topical editor of the *Journal of the Optical Society of America A*. Dr. Saleh is a Fellow of the Optical Society of America, a senior member of the Institute of Electrical and Electronics Engineers, and a member of Phi Beta Kappa and Sigma Xi. In 1984 he was appointed a Fellow of the John Simon Guggenheim Memorial Foundation.

M. C. Teich

M. C. Teich was born in New York City. He received the S.B. degree in physics from the Massachusetts Institute of Technology in 1961, the M.S. degree in electrical engineering from Stanford University in 1962, and the Ph.D. degree in quantum electronics from Cornell University in 1966. On graduating from Cornell, he joined the MIT Lincoln Laboratory, where he was engaged in work on coherent infrared detection. In 1967, he became a member of the faculty in the Department of Electrical Engineering at Columbia University, where he is now teaching and pursuing his research interests in the areas of photonics, quantum optics, lightwave communications, and sensory perception. He served as chairman of the department from 1978 to 1980. He is also a member of the faculty in the Department of Applied Physics and Nuclear Engineering and a member of the Columbia Radiation Laboratory, the Center for Telecommunications Research, and the Columbia Bioengineering Institute. Dr. Teich is a member of Sigma Xi, the American Physical Society, the Institute of Electrical and Electronics Engineers, the Acoustical Society of America, the Society for Neuroscience, the American Association for the Advancement of Science, and the New York Academy of Sciences. He served as a member of the Editorial Advisory Panel for *Optics Letters* from 1977 to 1979. In 1969 he was the recipient of the IEEE Browder J. Thompson Memorial Prize for his paper "Infrared Heterodyne Detection," and in 1981 he received the Citation Classic Award of *Current Contents* for this work. He was appointed a Fellow of the John Simon Guggenheim Memorial Foundation in 1973 and was elected a Fellow of the Optical Society of America in 1983.